

# The Heavy Hadron Spectrum

Christine Davies

Department of Physics and Astronomy, University of Glasgow, Glasgow, G12 8QQ,  
UK

**Abstract.** I discuss the spectrum of hadrons containing heavy quarks ( $b$  or  $c$ ), and how well the experimental results are matched by theoretical ideas. Useful insights come from potential models and applications of Heavy Quark Symmetry and these can be compared with new numerical results from the *ab initio* methods of Lattice QCD.

## 1 Introduction

The fact that we cannot study free quarks but only their bound states makes the prediction of the hadron spectrum a key element in testing Quantum Chromodynamics as a theory of the strong interactions. This test is by no means complete many years after QCD was first formulated.

The ‘everyday’ hadrons making up the world around us contain only the light  $u$  and  $d$  quarks. In these lectures, however, I concentrate on the spectrum of hadrons containing the heavy quarks  $b$  and  $c$  (the top quark is too heavy to have a spectrum of bound states, see for example Quigg (1997a)) because in many ways this is better understood than the light hadron spectrum, both experimentally and theoretically. The heavy hadrons only appear for a tiny fraction of a second in particle accelerators but they are just as important to our understanding of fundamental interactions as light hadrons. In fact the phenomenology of heavy quark systems is becoming very useful; particularly that of  $B$  mesons. The study of  $B$  decays and mixing will lead in the next few years, we hope, to a complete determination of the elements of the Cabibbo-Kobayashi-Maskawa matrix to test our understanding of CP violation. CKM elements refer to weak decays from one quark flavour to another but the only measurable quantity is the decay rate for hadrons containing those quarks. To extract the CKM element from the experimental decay rate then requires theoretical predictions for the hadronic matrix element. We cannot expect to get these right if we have not previously matched the somewhat simpler theoretical predictions for the spectrum to experiment.

Here I will review the current situation for the spectrum of bound states with valence heavy quarks alone and bound states with valence heavy quarks and light quarks. The common thread is, of course, the presence of the heavy quark, but we will nevertheless find a very rich spectrum with plenty of variety in theoretical expectations and phenomenology. A lot of the recent theoretical progress has been made using the *ab initio* techniques of Lattice QCD. These are described elsewhere in this Volume ( Weingarten (1997)) along with recent results from Lattice QCD for the light hadron spectrum.

Quark model notation for the states in the meson spectrum will prove useful (baryons will not be discussed until section 3). The valence quark and anti-quark in the meson have total spin,  $S = 0$  or  $1$ , and relative orbital angular momentum,  $L$ . The total angular momentum, which becomes the spin of the hadron,  $\mathbf{J} = \mathbf{L} + \mathbf{S}$ . The meson state is then denoted by  $n^{2S+1}L_J$  where  $n$  is the radial quantum number.  $n$  is conventionally given so that the first occurrence of that  $L$  is labelled by  $n=1$  (i.e.  $n+1$  is the number of radial nodes).  $L = 0$  is given the name  $S$ ,  $L = 1$ , the name  $P$ , etc. To give  $J^{PC}$  quantum numbers for the state (the only physical quantum numbers) we need the facts that  $P = (-1)^{L+1}$  and, for  $C$  eigenstates,  $C = (-1)^{L+S}$ . In Table 1 a translation between  $n^{2S+1}L_J$  and  $J^{PC}$  is provided.

$n^{2S+1}L_J$	$J^{PC}$
$^1S_0$	$0^{-+}$
$^3S_1$	$1^{--}$
$^1P_1$	$1^{+-}$
$^3P_0$	$0^{++}$
$^3P_1$	$1^{++}$
$^3P_2$	$2^{++}$

**Table 1.**  $J^{PC}$  quantum numbers for quark model  $S$  and  $P$  states

The ordering of levels that we see in the meson spectrum (The Particle Data Group (1996)) is generally the naïve one i.e. that for a given combination of quark and anti-quark adding orbital or spin momentum or radial excitation increases the mass. This is clearer for the heavy hadrons since, because of their masses and properties, the quark assignments are unambiguous. For heavy hadrons it is also true, for reasons that I shall discuss, that the splittings between states of the same  $L$  but different  $S$  are smaller than the splittings between different values of  $L$  or  $n$ . To separate this fine structure from radial and orbital splittings it is convenient to distinguish spin splittings from spin-independent or spin-averaged splittings. Spin-averaged states are obtained by summing over masses of a given  $L$  and  $n$ , weighting by the total number of polarisations i.e  $(2J + 1)$ . Examples are given below - they will be denoted by a bar.

In Section 2 I begin with the phenomenology of mesons containing valence heavy quarks, the heavy-heavy spectrum. I shall discuss potential model approaches to predicting this spectrum as well as more direct methods recently developed in Lattice QCD. Section 3 will describe heavy-light mesons and baryons, both from the viewpoint of Heavy Quark Symmetry ideas and from Lattice QCD, using techniques successful in the heavy-heavy sector. Section 4 will give conclusions and the outlook for the future.

## 2 The Heavy-heavy Spectrum

Figure 1 shows experimental results for  $b\bar{b}$  and  $c\bar{c}$  bound states (The Particle Data Group (1996)). They have been fitted on to the same plot by aligning the spin-average of the  $1^3P_{0,1,2}$  states ( $\chi_b$  and  $\chi_c$ ). The spin-average  $\chi$  mass is defined by

$$M(\bar{\chi}) = \frac{1}{9} [M(^3P_0) + 3M(^3P_1) + 5M(^3P_2)] \quad (1)$$

and this has been set to zero in both cases. The overall scale of  $b\bar{b}$  meson masses is much larger than for  $c\bar{c}$  but we see that this simply reflects the larger mass of the  $b$  quarks. The lightest vector state for  $b\bar{b}$  is the  $\Upsilon$  produced in  $e^+e^-$  collisions with a mass of 9.46 GeV. Its radial excitations are known as  $\Upsilon'$  or  $\Upsilon(2S)$ ,  $\Upsilon''$  or  $\Upsilon(3S)$  and so on. The radial excitations are separated from the ground state by several hundred MeV. For  $c\bar{c}$  the lightest vector state is the  $J/\psi$  or  $\psi(1S)$  and this has a mass of 3.1 GeV. Its radial excitations are the  $\psi'$  or  $\psi(2S)$  and so on. Since the scale of Figure 1 spans 1 GeV it is clear that the splittings between states in both systems are very much smaller than the absolute masses of the mesons.

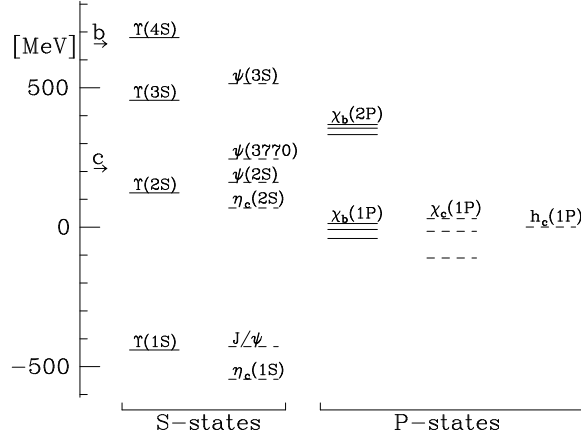


**Fig. 1.** The experimental heavy-heavy meson spectrum relative to the spin-average of the  $\chi_b(1P)$  and  $\chi_c(1P)$  states (The Particle Data Group (1996)).

It is also clear from Figure 1 that the radial excitations of the vector states in the two systems match each other very closely. In fact so closely that the

$\psi(3770)$  which has vector quantum numbers cannot be fitted into a scheme of radial excitations of the  $\psi$  system. It is thought to be not an  $S$  state but a  $D$  state (Rapidis *et al* (1977)). No  $b\bar{b}$   $D$  candidates have yet been seen).

The matching of radial excitations is even better if we consider spin-averaged  $S$  states,

$$M(\bar{S}) = \frac{1}{4} [M(^1S_0) + 3M(^3S_1)]. \quad (2)$$

The  $^1S_0$  state has only been seen for  $c\bar{c}$  and is denoted  $\eta_c$ . The  $\eta_c(^1S_0)$  lies below the vector state by 117 MeV and so the spin-average lies one quarter of this below the  $J/\psi$ . As we shall see, this spin splitting in the  $b\bar{b}$  system is expected to be much smaller. If we take a reasonable value for  $M(\Upsilon) - M(\eta_b)$  of 40-50 MeV (see later), we would find the  $1\bar{S}$  levels on Figure 1 to be aligned to within 10 MeV despite a difference in overall mass of a factor of 3. Similar arguments apply to the alignment of the  $2\bar{S}$  levels, although the agreement achieved there is not quite as good.

The spin splittings within the  $\chi_b(1P)$  states ( $\chi_{b0}, \chi_{b1}, \chi_{b2}$ ) are much smaller than those within the  $\chi_c(1P)$  states, so that the spin splittings do depend on the heavy quark mass,  $m_Q$ , quite strongly. For example, we can take the ratio for  $1P$  levels:

$$\frac{M(\chi_{b2}) - M(\chi_{b0})}{M(\chi_{c2}) - M(\chi_{c0})} = \frac{53 \text{ MeV}}{141 \text{ MeV}} = 0.38(1). \quad (3)$$

Näively this looks very similar to the ratio of  $b$  and  $c$  quark masses if we take these to be approximately half the mass of the vector ground states,  $\Upsilon$  and  $J/\psi$ . Then  $m_c/m_b \approx 0.33$ . This might imply a simple  $1/m_Q$  dependence for spin splittings. However, the ratio between  $b\bar{b}$  and  $c\bar{c}$  does depend somewhat on the splitting being studied, indicating a more complicated picture. We have :

$$\frac{M(\chi_{b1}) - M(\chi_{b0})}{M(\chi_{c1}) - M(\chi_{c0})} = 0.34(2), \quad (4)$$

and

$$\frac{M(\chi_{b2}) - M(\chi_{b1})}{M(\chi_{c2}) - M(\chi_{c1})} = 0.47(2). \quad (5)$$

The arrows shown on Figure 1 mark the minimum threshold for decay into heavy-light mesons,  $B\bar{B}$  for  $b\bar{b}$  and  $D\bar{D}$  for  $c\bar{c}$ . Three sets of  $S$  states and two sets of  $P$  states have been seen below this threshold for  $b\bar{b}$  and two sets of  $S$  states and one set of  $P$  states for  $c\bar{c}$ . Another set of  $P$  and two sets of  $D$  states are expected for  $b\bar{b}$  (Eichten (1980), Kwong and Rosner (1988)). The states below threshold are very narrow since the Zweig-allowed decay to heavy-light states (see Fig. 2) is kinematically forbidden and they must decay by annihilation. This carries a penalty of powers of the strong coupling constant,  $\alpha_s(M_Q)$ . These are then the states that we will concentrate on, because they can be treated as if they are stable (and none of the approaches which we will discuss allow them to decay). Vector states above threshold can still be seen in the  $e^+e^-$  cross-section as bumps but they are much broader and the theoretical understanding

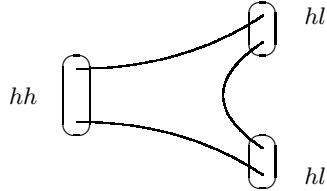


**Fig. 2.** Decay of a heavy-heavy meson to heavy-light mesons above threshold.

of their masses requires a model for the inclusion of decay channels in the analysis (Eichten *et al* (1978), Ono *et al* (1986)).

How can we understand the heavy-heavy spectrum below threshold? The fact that all the splittings are very much less than the masses, noted above, is critical. It implies that dynamical scales, such as the kinetic energy of the heavy quarks, are also very much less than the masses i.e. the quark velocities are non-relativistic,  $v^2 \ll c^2$ . Typical gluon momenta will be of the same order as typical quark momenta,  $m_Q v$ . Thus typical gluon energies,  $m_Q v$ , are very much larger than typical quark kinetic energies,  $m_Q v^2$  (Thacker and Lepage (1991)). The gluon interaction between heavy quarks will then appear ‘instantaneous’. It can be modelled using a potential and energies found by solving Schrödinger’s equation. In the extreme non-relativistic limit of very heavy quarks the spin splittings vanish. This was noticed above in the relation between  $b\bar{b}$  and  $c\bar{c}$  splittings and will be discussed in more detail later. In this limit we need only a single spin-independent central potential to solve for the spin-averaged spectrum of  $\bar{S}$  and  $\bar{P}$  states defined above. For a recent review of the history of the heavy quark potential see Quigg (1997b).

## 2.1 The spin-independent heavy quark potential

Perturbation theory for QCD gives a flavour-independent central potential based on 1-gluon exchange, which has a Coulomb-like form,

$$V(r) = -\frac{4}{3} \frac{\alpha_s}{r} \quad (6)$$

where  $r$  is the radial separation between the two heavy quarks and  $\alpha_s$  is the strong coupling constant. The Coulomb potential cannot be the final answer because it would allow free quarks to escape. In addition it gives a spectrum incompatible with experiment in which the  $1P$  level is degenerate with  $2S$ .

For a potential of the form  $V \sim r^{-N}$  with  $2 > N > 0$  we have a  $1P$  level below  $2S$ , as we observe, and a  $1D$  level above  $2S$  (as we see for charmonium).

So, the addition of some positive power of  $r$  to the Coulomb potential can rescue the phenomenology (Grosse and Martin (1980)). The additional term is usually taken to be linear in  $r$  and thought of as a ‘string-like’ confining potential. This gives the simple Cornell potential of Eichten *et al* (1975):

$$V(r) = -\frac{4}{3} \frac{\alpha_s}{r} + \sigma r \quad (7)$$

with  $\sigma$  called the ‘string tension’. This can reproduce the observed spectrum reasonably well. Other successful forms for the heavy quark potential are the Richardson potential (Richardson (1979)):

$$V(r) = \int d^3q e^{iq \cdot r} \frac{\alpha_s(q^2)}{4\pi q^2}, \quad (8)$$

in which a running strong coupling constant is included with non-perturbative behaviour at small  $q^2$  (see also Buchmüller and Tye (1981)), and the Martin potential (Martin (1980), Grant, Rosner and Rynes (1993)):

$$V(r) = Ar^\nu \text{ with } \nu \approx 0. \quad (9)$$

This last form, essentially a logarithmic potential (Quigg and Rosner (1977)), has no QCD motivation but is simply observed to work. All three potential forms can reproduce the  $b\bar{b}$  and  $c\bar{c}$  spin-averaged spectra reasonably well if the parameters are chosen appropriately. When this is done it is observed that the potentials themselves agree in the region  $r \sim 0.1 - 0.8$  fm in which the  $\sqrt{\langle r^2 \rangle}$  for the bound states sit (Buchmüller and Tye (1981)).

It is interesting to compare the dependence of the energies of the states on the mass of the heavy quark,  $m_Q$ , in different potentials. This can be done for homogeneous polynomial-type potentials easily (see, for example Quigg and Rosner (1979), Close (1979)). Schrödinger’s equation for the wavefunction  $\Psi$  is:

$$\left\{ -\frac{\hbar^2 \nabla^2}{2\mu} + V(r) \right\} \Psi(r) = E\Psi(r). \quad (10)$$

$E$  is the energy eigenvalue and  $\mu$ , the reduced mass,  $m_Q/2$  for the heavy-heavy case. For  $V = Ar^N$  we can reproduce the same solution at different values of  $m_Q$  if we allow for a rescaling  $r \rightarrow \lambda r$ . With this rescaling in place

$$\{-\hbar^2 \nabla^2 + A2\mu\lambda^{N+2}r^N\} \Psi(\lambda r) = 2\mu\lambda^2 E\Psi(\lambda r). \quad (11)$$

The same solution (with rescaled  $r$ ) will occur for different values of  $m_Q$  if

$$\lambda \propto \mu^{-1/(2+N)}. \quad (12)$$

This gives a solution for  $E$  which varies as

$$E \propto m_Q^{-N/(2+N)} \quad (13)$$

The values of  $E$  (and therefore splittings) will then be independent of  $m_Q$ , as observed approximately, for  $N = 0$ . This corresponds to the Martin potential. The same result can be achieved by mixing  $N = 1$  and  $N = -1$  in the Cornell potential. Note that the Feynman-Hellmann Theorem guarantees that bound states fall deeper into the potential as the mass increases,  $\partial E/\partial\mu < 0$  (Quigg and Rosner (1979)). For  $N > 0$ ,  $E$  falls with  $m_Q$ ; for  $N < 0$ ,  $E$  increases in the negative direction.

The Virial Theorem is helpful in extracting some dynamical parameters. It relates the mean kinetic energy to the expectation value of a derivative of the potential (see for example Quigg and Rosner (1979)):

$$\langle K \rangle = \frac{1}{2} \left\langle r \frac{dV}{dr} \right\rangle \quad (14)$$

for homogeneous potentials. For  $N \sim 0$  i.e.  $V \sim \log r$  we get  $K =$  a constant. Since

$$K = \frac{p^2}{2\mu} \quad (15)$$

this tells us that

$$\langle p^2 \rangle \propto \mu \quad (16)$$

and

$$v_{m_1}^2 = \frac{2\langle K \rangle m_2}{(m_1 + m_2)m_1} \quad (17)$$

for a meson made of different quarks of masses  $m_1$  and  $m_2$ .  $v_{m_i}$  is the velocity of the quark of mass  $m_i$  in the bound state. From fits using potential models a value of  $\langle K \rangle$  of 0.37 GeV is found (Quigg and Rosner (1979)), giving

$$c \text{ in } \psi, \frac{v^2}{c^2} \sim 0.24$$

$$b \text{ in } \Upsilon, \frac{v^2}{c^2} \sim 0.07$$

The quarks are non-relativistic as we originally expected. For the logarithmic potential we also have the result that  $v^2$  is independent of the radial excitation. For a Coulomb potential  $\langle p^2 \rangle$  decreases with increasing  $n$ , whereas for a linearly rising potential,  $\langle p^2 \rangle$  increases with increasing  $n$ .

Potential model calculations of the bottomonium and charmonium spectra are reasonably successful. See Eichten and Quigg (1994) for a recent example, whose results are plotted in Figure 3. These include not only the central (Richardson) potential discussed here but also (perturbative) spin-dependent potentials to be described in section 2.2 to get spin splittings. In Eichten and Quigg (1994) parameters of the potential were fixed from a subset of states in the experimental  $c\bar{c}$  spectrum. Typical deviations from experiment for the rest of the  $c\bar{c}$  spectrum were 30 MeV; typical deviations in the  $b\bar{b}$  spectrum were 25 MeV. Since the  $b$  quark is significantly more non-relativistic in its bound states than the  $c$  quark one might expect to get better agreement for the  $b\bar{b}$

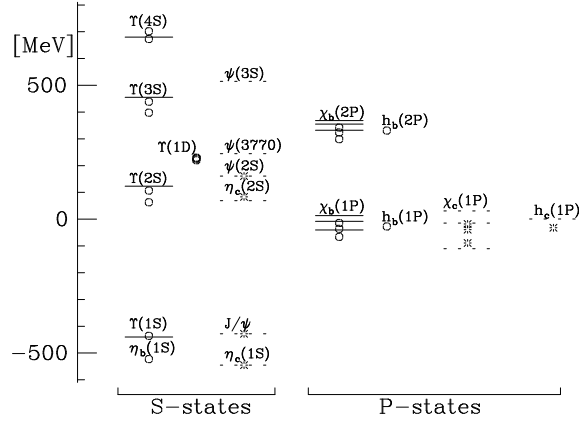


**Fig. 3.** The heavy-heavy meson spectrum from a recent Richardson potential model calculation (Eichten and Quigg (1994)). Circles and bursts show the calculated masses relative to the spin average of the  $\chi_b(1P)$  and  $\chi_c(1P)$  states and the solid and dashed lines show experiment results, where they exist.

spectrum using fitted parameters from that system. However, agreement for the  $c\bar{c}$  spectrum would then be worse. In either case it is necessary to fit the parameters of the phenomenological potential from some experimental information. Instead, the central potential  $V(r)$  can be extracted from first principles using the techniques of lattice QCD.

In the  $m_Q \rightarrow \infty$  limit the heavy quark is static. Its world line in space-time becomes a line of QCD gauge fields in the time direction. In Lattice QCD we break up space-time into a lattice of points and represent the gauge field by SU(3) matrices,  $U$  (Weingarten (1997), Montvay and Münster (1994)). The static quark propagator then becomes a string of  $U$  matrices, as in Figure 4.



**Fig. 4.** The world line of a heavy quark on the lattice.



We can put a quark and antiquark together and join them up into a closed, and therefore gauge-invariant loop, called a Wilson loop (Figure 5). The value of the Wilson loop can be measured on sets of gauge fields  $\{U\}$  where a gauge field is defined on every link of the lattice. These are called configurations. The physically useful quantity is the matrix element of the Wilson loop between vacuum states and this is obtained by averaging values of the Wilson loop over an ensemble of configurations where each configuration has been chosen as a typical snapshot of the vacuum of QCD. To obtain such an ensemble we must generate configurations with a probability weighting  $e^{-S_{QCD}}$  and there are standard techniques to do this (Weingarten (1997), Montvay and Münster (1994)).

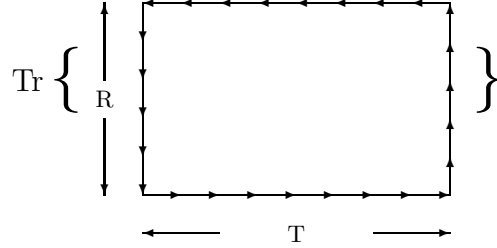


**Fig. 5.** A Wilson loop. The Trace is over colour indices.

The expectation value over such an ensemble of gauge fields of a Wilson loop of spatial size  $R$  is related to the heavy quark potential  $V(R)$ . This is because the ensemble average is a Monte Carlo estimate of the path integral giving the matrix element of the operator which creates and destroys a static heavy quark pair at separation  $R$  on the lattice. The matrix element becomes exponentially related to the ground state energy of the quark anti-quark pair as the time extent of the Wilson loop,  $T$ , tends to infinity. Since  $R$  is fixed, and the quarks in this picture have no kinetic energy, this is simply the potential  $V(R)$  plus an additive self-energy contribution.

$$\begin{aligned}
 \langle \text{Wilson Loop} \rangle &= \frac{\int \mathcal{D}U \text{Wilson Loop}(U) e^{-S_{QCD}}}{\int \mathcal{D}U e^{-S_{QCD}}} & (18) \\
 &= \langle 0 | [\psi^\dagger(0) \chi^\dagger(R)]_{t=0} [\psi(0) \chi(R)]_{t=T} | 0 \rangle \\
 &\xrightarrow{T \rightarrow \infty} |\langle 0 | \psi(0) \chi(R) | \text{ground state} \rangle|^2 e^{-ET} + \text{higher order terms} \\
 E = V_{latt}(R) &= V(R) + \text{constant}.
 \end{aligned}$$

How is the calculation done? Once the ensemble of gauge field configurations has been generated, Wilson loops of various different sizes in  $R$  and  $T$  are measured and average values of  $W(R, T)$  obtained. There is a statistical error associated with the number of configurations in the ensemble, i.e. how good an estimate of the path integral has been obtained. For a fixed  $R$ ,  $W(R, T)$  is fitted to the exponential form above in the large  $T$  limit, extracting  $E$ . Away from  $T = \infty$  higher order terms should be included in the fit which are exponentials of excitations of the potential. There are a number of techniques to improve the values of  $E$  obtained, both the statistical error and any systematic error from fitting to an exponential form (see, for example, Bali, Schilling and Wachter (1997a)). Several of the techniques are similar to those used in direct calculations of the spectrum and are discussed in section 2.3.

Once  $V_{latt}(R)$  is obtained it can either be used directly or a functional form in terms of  $R$  can be extracted to inform the continuum potential model approaches described above. The functional form usually used is that of the Cornell potential with  $e = 4\alpha_s/3$  and an additive constant,  $V_c$ :

$$V_{latt}(R) = \sigma R - \frac{e}{R} + V_c. \quad (19)$$

The fit then yields the parameters  $\sigma$ ,  $e$  and  $V_c$ .  $e$  is generally taken as a constant, although it is possible to determine the running coupling constant  $\alpha_s(R)$  from the short distance potential (UKQCD (1992b)). Often the running is mimicked by keeping  $e$  constant and adding an additional term,  $f/R^2$ . This affects slightly the value of  $e$  obtained, as does the range of  $R$  included in the fit. A Martin form plus a constant, equation 9, does not fit  $V_{latt}$  (Bali, private communication).

It is important to remember that  $V_{latt}$ , being obtained from the lattice, is measured in lattice units. To convert to dimensionful units of GeV we need to know the lattice spacing,  $a$ . This requires one piece of experimental information (see below). The separation,  $R$ , is also measured in lattice units, corresponding to a physical distance  $r = Ra$  in fm. Thus the continuum potential  $V$  is obtained by

$$V(r = Ra) = V_{latt}(R) \times a^{-1} \quad (20)$$

However this expression should contain on the r.h.s. only the physical pieces of  $V_{latt}$  and not  $V_c$ .

$V_c$  is an unphysical constant which resets the zero of energy. It arises from corrections to the static quark self-energy induced by gluon loops sitting around the perimeter of the Wilson loop. These give a contribution to the logarithm of the Wilson loop proportional to its perimeter,  $V_c(2R + 2T)/2$ . Thus the term  $V_c$  appears as part of  $V_{latt}$ . In perturbation theory  $V_c$  is a power series in the coupling constant  $\alpha_s$ , starting at  $\mathcal{O}(\alpha_s)$ , but is otherwise a constant in lattice units. From equation 20, its contribution to the continuum potential diverges on the approach to the continuum limit,  $a \rightarrow 0$ , and it should be subtracted from  $V_{latt}$  before equation 20 is applied. Another way to look at this is to notice that the heavy quark potential on the lattice is forced to zero at zero separation,  $V_{latt}(0) = 0$ , when the Wilson loop collapses to two lines on top of one another. Because the

$U$  matrices are unitary we get  $\langle \text{WilsonLoop} \rangle = 1 = e^0$ . However, the continuum potential diverges in Coulomb fashion at zero separation so that  $V(0)a \neq 0$ . The physical pieces of the lattice potential will reproduce the continuum behaviour so to get  $V_{latt}(0) = 0$  will require an additive constant to shift the whole potential upwards. This is  $V_c$ .

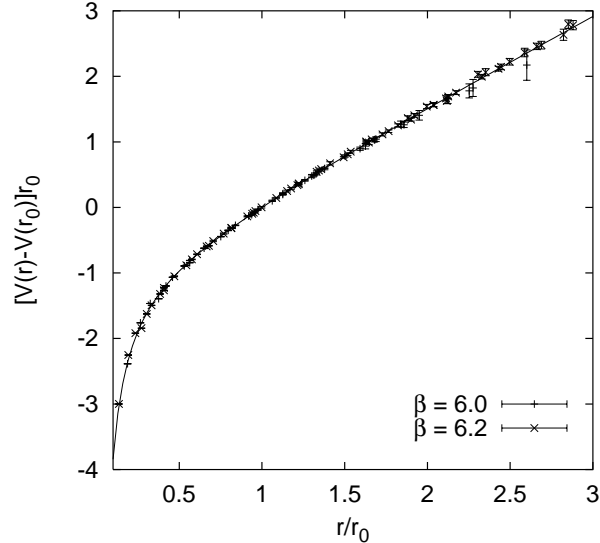


**Fig. 6.** The heavy quark potential obtained from the lattice at two different values of the lattice spacing in the quenched approximation. The solid line is a fit of the form 19 (Bali, Schilling and Wachter (1997a)). The potential and separation are given in units of the parameter  $r_0$  (see text).

Figure 6 shows recent results for the lattice potential plotted with the fitted form above, (19). The parameters extracted can be compared to those of phenomenological potentials.

The Coulomb coefficient,  $e$ , is dimensionless and needs no multiplication by powers of the inverse lattice spacing to get a physical result.  $e$  is the coefficient of the  $1/R$  term but the discrete nature of the lattice changes

$$\frac{1}{R} \rightarrow \frac{4\pi}{L^3} \sum_{q \neq 0} \frac{e^{iq \cdot R}}{\sum_i \hat{q}_i^2}, \quad \hat{q}_i^2 = 2 \sin \frac{q_i}{2} \quad (21)$$

Notice that this lattice form of  $1/R$  is not rotationally invariant. At finite lattice spacing there are two alternatives. One is to fit this modified ‘lattice’ form of

$1/R$ ; the other is to correct for the discretisation errors in the naïve lattice action,  $S_{QCD}$  which gave rise to them (Lepage (1996)).

Most precision lattice calculations of the heavy quark potential have worked in the quenched approximation in which only the gluonic terms are included in  $S_{QCD}$ . This is equivalent to ignoring quark-antiquark pairs popping in and out of the vacuum (Weingarten (1997), Montvay and Münster (1994)). Recent calculations (Bali, Schilling and Wachter (1997a), Bali and Schilling (1992), UKQCD (1992a)) have given a value of  $e$  around 0.3, which is rather smaller than the values that phenomenological potentials have used. For example, Eichten and Quigg (1994) use  $e = 0.54$  in their Cornell potential fits. Part of this discrepancy can be traced to errors in the quenched approximation. When no  $q\bar{q}$  pairs are available in the vacuum for screening, the strong coupling constant will run to zero too fast at small distances. Thus

$$\begin{aligned}\alpha_s(r)_{Q.A.} &< \alpha_s(r)_{\text{full theory}} \\ V(r)_{Q.A.} &> V(r)_{\text{full theory}}\end{aligned}$$

when  $V(r)$  is dominated by the Coulomb term. Calculations of the heavy quark potential that have been done on unquenched configurations (which usually contain two flavours of degenerate massive quarks in the vacuum, still not entirely simulating the real world), indicate that  $e$  is increased by about 10%. This gives a steeper potential at short distances, as in Figure 7. SESAM (1996) find  $e_{Q.A.} = 0.289(55)$  and  $e_{unquenched} = 0.321(100)$  without the use of the  $f/R^2$  term in Equation 19. This doesn't then explain all of the difference between lattice values of  $e$  and phenomenological continuum values.

Phenomenological potentials also implicitly include some relativistic corrections to the static picture that can be modelled simply as  $r$ -dependent additional potentials. The first such corrections contain a term inversely proportional to the square of the heavy quark mass multiplying a Coulomb potential, and therefore altering the effective value of  $e$  in an  $m_Q$ -dependent way. The coefficient of these corrections can be calculated on the lattice (Bali, Schilling and Wachter (1997a)). It is found that  $e$  becomes  $e + b/m_Q^2$  where  $b = (0.86(5)\text{GeV})^2$ , giving a significant increase (35%) to the effective value of  $e$  for charmonium but no change for bottomonium. This is illustrated in Figure 8, and supports the phenomenological use of different values for  $e$  in the two systems as a flavour-dependent dynamical effect.

The string tension,  $\sigma$ , describes the strength of the linearly rising part of the potential. It is dimensionful, so  $\sigma_{latt} = \sigma a^2$ . Using values of  $\sigma$  from phenomenological potentials (Eichten and Quigg (1994) use  $\sqrt{\sigma} \approx 0.43 \text{ GeV}$ ) allows us to fix  $a$  on the lattice and then convert all other dimensionful quantities to physical units. However,  $\sigma$  and  $e$  are anti-correlated from the fitted form used in equation 19 and this gives some bias. It is better to use instead the value  $r_0$  obtained by setting  $r^2 F(r)$  to a fixed value.  $F(r)$  is the interquark force, obtained by differentiating the potential, and a suitable fixed value is 1.65 which corresponds to  $r_0 \approx 0.5 \text{ fm} (\equiv 2.5\text{GeV}^{-1}$  when  $\hbar c = 1$ ) (Sommer (1994)). Ensembles at different

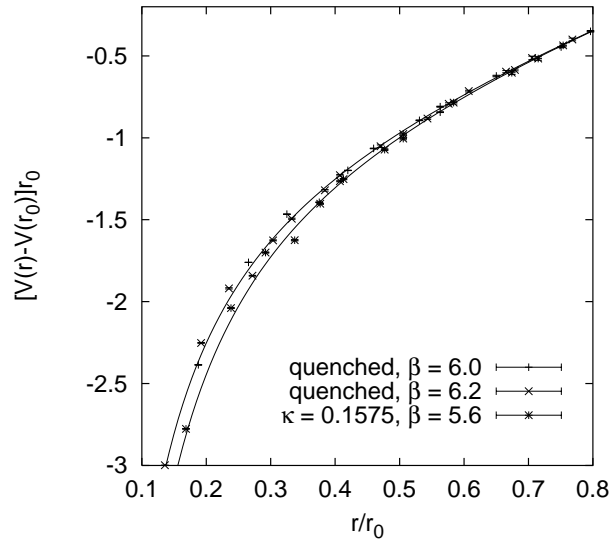


**Fig. 7.** A comparison of the short-distance heavy quark potential obtained from the lattice on quenched and unquenched configurations by the SESAM collaboration. The potential and separation are given in units of the parameter  $r_0$  (see text). Figure provided by Gunnar Bali.

values of  $a$  are obtained by using different bare coupling constants in the action,  $S_{QCD}$  (Weingarten (1997), Montvay and Münster (1994)). However, the value of  $a$  for a given value of the bare coupling constant is not known *a priori* but has to be obtained by calculating a dimensionful parameter and comparing to experiment (or, in the case of  $\sigma$  or  $r_0$  above, to phenomenology). Fixing  $a$  is a critical step in a lattice calculation and introduces additional systematic and statistical errors into the quoted physical results. In the quenched approximation the value of  $a$  for a given gauge coupling,  $\beta$ , will depend on the experimental quantity chosen to fix it, and so it is important to know what quantity was chosen when looking at lattice results. This point will be discussed further later.

Given a value for  $a$ ,  $V_{latt} - V_c$  can be converted to GeV at separations,  $r$ , in fm ( $\equiv \text{GeV}^{-1}$ ). This is then the physical heavy quark potential and it should be independent of the lattice spacing at which the calculation was done. Figure 6 shows that this is true for current lattice results.

Using the fitted form for the potential, the spectrum can be calculated by solving Schrödinger's equation in the continuum (Bali, Schilling and Wachter (1997a)). The heavy quark mass and the overall scale (given by the string tension) need to be adjusted to optimise the fit to experiment. Including the relativistic corrections to the potential described above and adjusting the value of

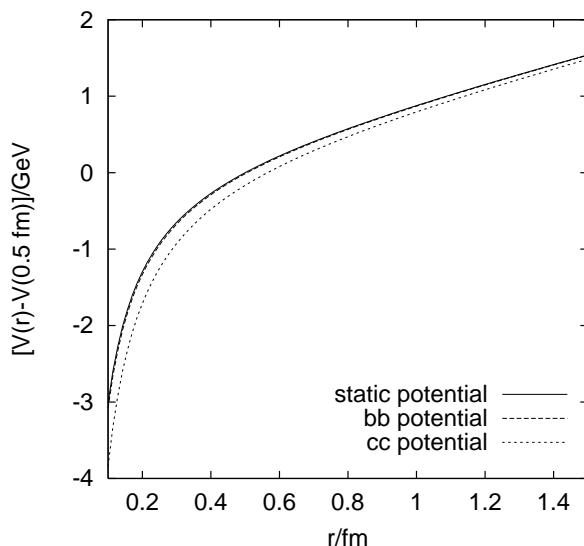


**Fig. 8.** A comparison of the heavy quark potential obtained from the lattice including the first relativistic corrections which yield an  $m_Q$ -dependent Coulomb term. The static ( $m_Q \rightarrow \infty$ ) potential is given by the solid line and those for  $b$  and  $c$  by dashed lines. Figure provided by Gunnar Bali, see Bali, Schilling and Wachter (1997a).

$e$  to mimic an unquenched result, yields average deviations from experiment of around 10 MeV for bottomonium and rather larger, as expected, 20 MeV for charmonium. The remaining systematic errors in the lattice potential (see section 2.2) could cause shifts of this size for bottomonium and make the 20 MeV deviations for charmonium look rather fortuitous.

**Exercise:** Discuss how you would expect the potential appropriate to heavy baryons to behave. How would you calculate this on the lattice? (Thacker, Eichten and Sexton (1988)).

## 2.2 The spin-dependent heavy quark potential

As described above, the infinitely massive heavy quark is only a colour source; it carries no spin. To obtain spin splittings then we must move away from the static picture. A useful starting point is a non-relativistic expansion of the Dirac Lagrangian which is appropriate for heavy quarks in heavy-heavy systems (Thacker and Lepage (1991)). This can be obtained by a Foldy-Wouthuysen-Tani transformation of the Dirac Lagrangian in Euclidean space (see for example Itzykson

and Zuber (1980)):

$$\begin{aligned}
 \mathcal{L} = \psi^\dagger & \left( D_t - \frac{\mathbf{D}^2}{2m_Q} \right. \\
 & - c_1 \frac{(\mathbf{D}^2)^2}{8m_Q^3} + c_2 \frac{ig}{8m_Q^2} (\mathbf{D} \cdot \mathbf{E} - \mathbf{E} \cdot \mathbf{D}) \\
 & \left. - c_3 \frac{g}{8m_Q^2} \boldsymbol{\sigma} \cdot (\mathbf{D} \times \mathbf{E} - \mathbf{E} \times \mathbf{D}) - c_4 \frac{g}{2m_Q} \boldsymbol{\sigma} \cdot \mathbf{B} \dots \right) \psi.
 \end{aligned} \tag{22}$$

$\psi$  is a 2-component spinor with heavy quark and anti-quark decoupled. The mass term  $\psi^\dagger m_Q \psi$  has been dropped.  $\mathbf{D}$  is a covariant derivative coupling to the gluon field and  $\mathbf{E}$  and  $\mathbf{B}$  are chromo-electric and chromo-magnetic fields. The rest of the QCD Lagrangian for light quarks and gluons remains as usual.

The terms in the Lagrangian can be ordered in powers of the squared velocity of the heavy quark using the following power counting rules for momentum and kinetic energy (Lepage *et al* (1992), Bodwin *et al* (1995)):

$$\begin{aligned}
 \mathbf{D} & \sim p \sim m_Q v \\
 K & \sim m_Q v^2
 \end{aligned}$$

Then from the lowest order field equation

$$\left( \partial_t - igA_4 - \frac{\mathbf{D}^2}{2m_Q} \right) \psi = 0 \tag{23}$$

we have

$$\begin{aligned}
 gA_4 & \sim \partial_t \sim K = m_Q v^2 \\
 g\mathbf{E} & = [D_t, \mathbf{D}] \sim pK = m_Q^2 v^3 \\
 -ig\epsilon_{ijk} B^k & = [D_i, D_j] \sim K^2 = m_Q^2 v^4.
 \end{aligned}$$

In  $\mathcal{L}$  we then see that the leading order terms on the first line of equation 22 are  $\mathcal{O}(m_Q v^2)$  and these give spin-independent splittings in the heavyonium spectrum. On the second line are spin-independent terms of  $\mathcal{O}(m_Q v^4)$  which are relativistic corrections to the leading terms. On the third line are spin-dependent terms also of  $\mathcal{O}(m_Q v^4)$ . These are the leading terms as far as spin-splittings are concerned. So, as discussed earlier, spin splittings should be  $\mathcal{O}(v^2)$  times smaller than spin-independent splittings. This is equivalent to  $1/m_Q$  behaviour, with a roughly constant kinetic energy, giving around 120 MeV for  $c\bar{c}$  and 40 MeV for  $b\bar{b}$ . Note that the  $\boldsymbol{\sigma} \cdot (\mathbf{D} \times \mathbf{E})$  and  $\boldsymbol{\sigma} \cdot \mathbf{B}$  spin-dependent terms are of the same order because the chromo-magnetic field is suppressed by one power of  $v$  over the chromo-electric field in the power counting.

Following these power-counting rules the number of operators to be included in  $\mathcal{L}$  can be truncated at a fixed order in  $v^2/c^2$  and this is obviously a sensible thing to do if  $v^2/c^2 \ll 1$ . In describing heavy-heavy systems with this

Lagrangian, however, we have lost the renormalisability of QCD. To obtain useful results we must put in a cut-off,  $\Lambda$ , to restrict momenta to  $p < \Lambda < m_Q$ . The excluded momenta e.g. in gluon loops will reappear as a renormalisation of the coefficients of the non-relativistic operators, the  $c_i$  of equation 22. The  $c_i$  can be calculated in perturbation theory (since they are dominated by ultra-violet scales for  $\Lambda \gg \Lambda_{QCD}$ ) by matching low energy scattering amplitudes of (22) to full QCD to some order in  $\alpha_s$  and  $p/m_Q$ . The  $c_i$  are all one at tree-level.

I will describe two different, but related, approaches to the study of spin splittings in heavyonium. One is to take  $\mathcal{L}$  of equation 22 and discretise it directly on the lattice - this is the NonRelativistic QCD approach (Thacker and Lepage (1991)). The second is to develop spin-dependent potentials from  $\mathcal{L}$  to add into a Schrödinger equation,  $H\psi = E\psi$ , and solve for the splittings.

$$H = \sum_{i=1}^2 \left\{ \frac{\mathbf{p}^2}{2m_i} - c_1 \frac{\mathbf{p}^4}{8m_i^3} \right\} + V_o(r) + V_{sd}(r, \mathbf{L}, \mathbf{S}_1, \mathbf{S}_2) \quad (24)$$

where  $V_0(r)$  is the central potential from section 2.1 and  $V_{sd}$  includes the spin-dependent potentials. Again one can take a phenomenological approach to the spin-dependent potentials, or extract them from the lattice. I will describe the potential approach first and then return to NRQCD in the next subsection.

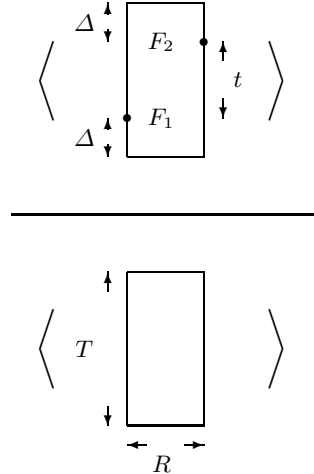


**Fig. 9.** The ratio of expectation values required for the spin-dependent potentials.  $F_1$  and  $F_2$  represent insertions of  $E$  or  $B$  as required for that potential. For some potentials these will be on the same side of the Wilson loop. The distance  $\Delta$  should be large and  $t$  is summed over (see text).

To extract spin-dependent potentials from QCD we start from the Wilson



loop which represents a static quark anti-quark pair at separation  $R$  (Eichten and Feinberg (1981), Peskin (1983)). As discussed earlier, the heavy quark propagator in this case is simply a line in the time direction, from the simplest possible heavy quark Lagrangian,  $\psi^\dagger D_t \psi$ . Imagine adding a perturbation  $\boldsymbol{\sigma} \cdot \mathbf{B}/2m_Q$  to the quark or anti-quark, such as would come from relativistic corrections to the propagator using the Lagrangian of equation 22. On one leg alone, zero is obtained by symmetry. If the perturbation is added to both legs and we sum over the time separations,  $t$ , between the two additions a new contribution to the potential is obtained of the form  $\mathbf{S}_1 \mathbf{S}_2 \Delta V/m_{Q1} m_{Q2}$ .

$$\Delta V = 2 \lim_{\tau \rightarrow \infty} \int_0^\tau dt \langle \langle B(\mathbf{0}, 0) B(\mathbf{R}, t) \rangle \rangle_W \quad (25)$$

where  $\langle \langle \rangle \rangle_W$  means the expectation value in the presence of the Wilson loop i.e. the ratio of the expectation value of the Wilson loop with the  $B$  field insertions to that without. This is easy to calculate using the methods of Lattice QCD (Michael and Rakow (1985), de Forcrand and Stack (1985)). Figure 9 illustrates this ratio for one value of  $t$ . An integration over  $t$  is required and this is approximated on the lattice by a sum (see Bali, Schilling and Wachter (1997a) for a recent description of the techniques used). The time separations of the insertion points from the ends of the Wilson loop,  $\Delta$ , must be kept large to ensure that the spin-dependent contribution to the static propagation of a  $Q\bar{Q}$  pair is obtained in the ground state of the central potential; excited states must have time to decay away.

The complete spin-dependent potential is given by (Eichten and Feinberg (1981), Chen, Kuang and Oakes (1995)):

$$\begin{aligned} V_{sd} = & \frac{1}{2r} \left( \frac{\mathbf{S}_1}{m_{Q1}^2} + \frac{\mathbf{S}_2}{m_{Q2}^2} \right) \cdot \mathbf{L} \left[ d_0 V_0'(r) + 2d_1 V_1'(r) \right] \quad (26) \\ & + \frac{1}{r} \left( \frac{\mathbf{S}_1 + \mathbf{S}_2}{m_{Q1} m_{Q2}} \right) \cdot \mathbf{L} d_2 V_2'(r) \\ & + \left( \frac{\mathbf{S}_1 \cdot \mathbf{r} \mathbf{S}_2 \cdot \mathbf{r}}{m_{Q1} m_{Q2} r^2} - \frac{1}{3} \frac{\mathbf{S}_1 \cdot \mathbf{S}_2}{m_{Q1} m_{Q2}} \right) d_3 V_3(r) \\ & + \frac{\mathbf{S}_1 \cdot \mathbf{S}_2}{3m_{Q1} m_{Q2}} d_4 V_4(r) \\ & + \frac{1}{r} \left( \frac{\mathbf{S}_1}{m_{Q1}^2} - \frac{\mathbf{S}_2}{m_{Q2}^2} \right) \cdot \mathbf{L} \tilde{d}_0 \left[ V_0'(r) + V_1'(r) \right] \\ & + \frac{1}{r} \left( \frac{\mathbf{S}_1 - \mathbf{S}_2}{m_{Q1} m_{Q2}} \right) \cdot \mathbf{L} \tilde{d}_2 V_2'(r) \end{aligned}$$

The primes indicate differentiation with respect to the argument  $r$  of the different potentials. Note that the last two terms appear only for the unequal mass case. The  $d_i$  and  $\tilde{d}_i$  coefficients will be discussed below. In perturbation theory the  $d_i$  coefficients appear at  $\mathcal{O}(1)$ , the  $\tilde{d}_i$  only at  $\mathcal{O}(\alpha_s)$  and only for

$m_{Q1} \neq m_{Q2}$ .  $V_0$  is the central potential, discussed in section 2.1, and  $V_1$ ,  $V_2$ ,  $V_3$ ,  $V_4$  are obtained on the lattice by calculating the following expectation values:

$$\frac{R_k}{R} V_1'(R) = 2\varepsilon_{ijk} \lim_{\tau \rightarrow \infty} \int_0^\tau dt t \left\langle \begin{array}{c} E_j \\ B_i \end{array} \right\rangle / Z_W \quad (27)$$

$$\frac{R_k}{R} V_2'(R) = \varepsilon_{ijk} \lim_{\tau \rightarrow \infty} \int_0^\tau dt t \left\langle \begin{array}{c} E_j \\ B_i \end{array} \right\rangle / Z_W \quad (28)$$

$$[\hat{R}_i \hat{R}_j - \frac{1}{3} \delta_{ij}] V_3(R) + \frac{1}{3} \delta_{ij} V_4(R) = 2 \lim_{\tau \rightarrow \infty} \int_0^\tau dt \left\langle \begin{array}{c} B_j \\ B_i \end{array} \right\rangle / Z_W \quad (29)$$

As in Figure 9, the denominator  $Z_W$  is the expectation of the Wilson loop without  $E$  or  $B$  field insertions.

A lattice discretisation of the  $E$  and  $B$  field strength operators is required. The simplest discretisation of  $F_{\mu\nu}(\mathbf{x})$  is to take the product of four  $U$  matrices around a  $1 \times 1$  square in the  $\mu, \nu$  plane starting from the corner  $\mathbf{x}$ . This product is called a plaquette (Weingarten (1997), Montvay and Münster (1994)); its hermitian conjugate should be subtracted and the resulting  $SU(3)$  matrix made traceless. Note that factors of  $g$  that would otherwise appear from equation 22 are absorbed into the lattice version of  $F_{\mu\nu}$ . For the  $B$  field, a more symmetric version of this is to use, instead of one plaquette, the average of the four plaquettes around point  $\mathbf{x}$  in the spatial plane perpendicular to  $\mathbf{B}$  (see Figure 10). For  $\mathbf{E}$  the spatial average of the two plaquettes at a given time is used. See Bali, Schilling and Wachter (1997a) for details.

The central potential, as calculated on the lattice, is a spectral quantity, appearing in the exponent of the exponential decay of a correlation function. It can therefore be directly interpreted as the continuum potential once converted to physical units. The spin-dependent potentials, in contrast, are calculated from the amplitudes of lattice correlation functions and undergo renormalisation when compared to continuum QCD. This renormalisation is visible in equation 26 as the  $d_i$  coefficients. These are functions of the  $c_i$  coefficients since the potentials are extracted by perturbing the Wilson loop with operators from equation 22 (Chen, Kuang and Oakes (1995)). They reflect the matching required between

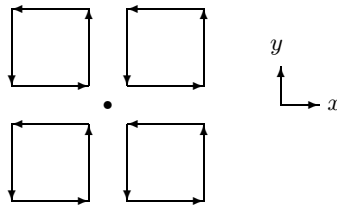


**Fig. 10.** The sum of four untraced plaquettes around a point (the clover-leaf operator) that is used for a  $B_z$  field insertion in a wilson loop for spin-dependent potentials (see text).

this static/nonrelativistic effective theory and full QCD. In this case it is convenient to do the matching in two stages; full QCD to continuum effective theory and continuum effective theory to lattice effective theory.

For the first stage the  $c_i$  (and therefore  $d_i$ ) have been calculated in leading order continuum perturbation theory (Eichten and Hill (1990), Falk, Grinstein and Luke (1991)). They depend logarithmically on the quark mass and the cut-off that is applied to the effective theory. The spin-dependent potentials also depend on the cut-off, but not  $m_Q$ , so that each term in  $V_{sd}$  becomes

$$d_i(A, m_Q)V_i(A). \quad (30)$$

We can use the  $d_i$  calculated in the continuum for the lattice calculation if we imagine the continuum effective theory at the same cut-off as the lattice cut-off ( $1/a$ ).

For the second stage we then match between continuum and lattice effective theories at the same cut-off. This provides an additional renormalisation which can be significant because of the non-linear relationship between the continuum and lattice gauge fields (Lepage and Mackenzie (1993)). This gives rise to additional tadpole diagrams in lattice perturbation theory. They have a universal nature and can be thought of (even beyond perturbation theory) as a constant factor multiplying each gauge link. Equivalently the renormalisation can be viewed as arising from the additional perimeter self-energy contributions when the  $E$  and  $B$  field insertion are in place (de Forcrand and Stack (1985)). A method to take account of the renormalisation directly on the lattice involves calculating, instead of the ratio in Figure 9, the product of ratios in Figure 11 (Huntley and Michael (1987)). The additional perimeter/tadpole terms from the insertions are thereby cancelled out, and it is hoped that any remaining lattice renormalisation is negligible.

Once the spin-dependent potentials are calculated from Figure 11 and multiplied by the appropriate  $d_i$ , they can be inserted into a Schrödinger equation and the energy shifts from the spin-independent states can be calculated (Bali, Schilling and Wachter (1997a)). They depend on the functional form of the spin-dependent potentials and on the expectation value of the spin and orbital angular

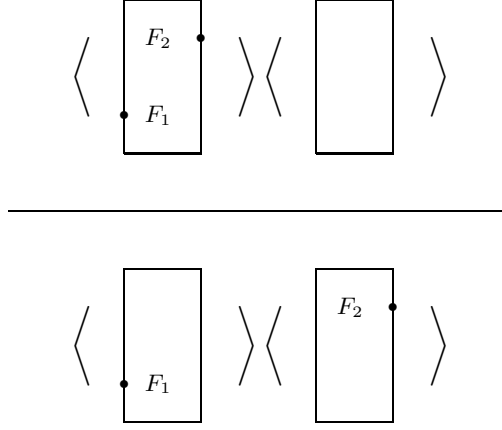


**Fig. 11.** The ratio of expectation values used for the spin-dependent potentials, taking account of renormalisation required to match to the continuum (Huntley and Michael (1987)).  $F_1$  and  $F_2$  represent insertions of  $E$  or  $B$  as required for that potential.

momentum operators of equation 26 for a particular state. To calculate these the following equations are useful (for the last relation see Kwong and Rosner (1988)):

$$\begin{aligned}
 \langle \mathbf{S}_1 \cdot \mathbf{S}_2 \rangle &= \frac{1}{2} \left[ S(S+1) - \frac{3}{2} \right] & (31) \\
 \langle \mathbf{L} \cdot \mathbf{S}_1 \rangle &= \langle \mathbf{L} \cdot \mathbf{S}_2 \rangle = \frac{1}{2} \langle \mathbf{L} \cdot \mathbf{S} \rangle \\
 \langle \mathbf{L} \cdot \mathbf{S} \rangle &= \frac{1}{2} [J(J+1) - L(L+1) - S(S+1)] \\
 \langle S_{ij} \rangle &= 4 \langle 3(\mathbf{S}_i \cdot \hat{\mathbf{n}})(\mathbf{S}_j \cdot \hat{\mathbf{n}}) - \mathbf{S}_i \cdot \mathbf{S}_j \rangle \\
 &= 2 \langle 3(\mathbf{S} \cdot \hat{\mathbf{n}})(\mathbf{S} \cdot \hat{\mathbf{n}}) - \mathbf{S}^2 \rangle \\
 &= - \frac{[12 \langle \mathbf{L} \cdot \mathbf{S} \rangle^2 + 6 \langle \mathbf{L} \cdot \mathbf{S} \rangle - 4S(S+1)L(L+1)]}{(2L-1)(2L+3)}
 \end{aligned}$$

The results for the expectation values are tabulated for  $S$  and  $P$  states in Table 2. It is clear from this table that the only potential contributing to the hyperfine splitting between the  $^3S_1$  and  $^1S_0$  states ( $M(\Upsilon) - M(\eta_b)$ ,  $M(J/\Psi) - M(\eta_c)$ ) is  $V_4$ . For the splittings between  $P$  states, all the spin-spin and spin-orbit potentials can contribute in principle. Notice how the spin-averaging described at the beginning of section 2 removes all the spin-dependent pieces, to obtain the spin-independent spectrum. To remove  $V_4$  terms from  $P$  states the spin-average must be taken including the  $^1P_1$ .

	$^1S_0$	$^3S_1$	$^1P_1$	$^3P_0$	$^3P_1$	$^3P_2$
$\langle \mathbf{S}_1 \cdot \mathbf{S}_2 \rangle$	$-\frac{3}{4}$	$\frac{1}{4}$	$-\frac{3}{4}$	$\frac{1}{4}$	$\frac{1}{4}$	$\frac{1}{4}$
$\langle \mathbf{L} \cdot \mathbf{S} \rangle$	0	0	0	-2	-1	1
$\langle S_{ij} \rangle$	0	0	0	-4	2	$-\frac{2}{5}$

**Table 2.** Expectation values for combinations of spin and orbital angular momentum operators needed for spin splittings in heavy-heavy bound states.

What functional form do we expect for the different spin-dependent potentials? In leading order perturbation theory (one gluon exchange):

$$\begin{aligned}
 V_0 &= -C_F \frac{\alpha_s}{r} & (32) \\
 V_1' &= 0 \\
 V_2' &= C_F \frac{\alpha_s}{r^2} \\
 V_3 &= 3C_F \frac{\alpha_s}{r^3} \\
 V_4 &= 8\pi C_F \alpha_s \delta^{(3)}(r),
 \end{aligned}$$

with  $C_F = 4/3$ . The ‘same-side’ (see equation 27) spin-orbit interaction,  $V_1$ , is absent; the ‘opposite-side’,  $V_2$  is simply  $V_0$ . The form of  $V_4$  implies that it is only effective for states with a wavefunction at the origin i.e.  $S$  states. It gives for the  $^3S_1 - ^1S_0$  splitting,

$$\frac{32\pi\alpha_s}{9m_Q^2} |\psi(0)|^2. \quad (33)$$

We do not then expect any splitting induced by the  $V_4$  term between the  $^1P_1$  and  $^3P_1$  states, so the  $^1P_1$  mass should be at the spin-average of the  $^3P$  states.

The following inter-relationships between potentials are also useful.

$$V_2' - V_1' = V_0' \quad (34)$$

$$V_3(r) = \frac{V_2'(r)}{r} - V_2''(r) \quad (35)$$

$$V_4(r) = 2\nabla^2 V_2(r) \quad (36)$$

Equation 34 is the Gromes relation (Gromes (1984)), derived from Lorentz invariance and as such always true. Equations 35 and 36 hold for any vector-like exchange (such as single gluon) but only to leading order; they do not survive renormalisation of the potentials when the cut-off on the effective Lagrangian of equation 22 is changed. In particular  $V_1$  and  $V_2$  then mix (Chen, Kuang and Oakes (1995)).

A crucial ingredient missed in the perturbative analysis is the confining part of the central potential,  $V_0$ , and this can reappear in the  $V_i$ . The nature of this

confining term is important. General considerations (Gromes (1977)) show that it can only arise from vector and/or scalar exchange, but these two possibilities yield quite different accompanying spin-dependent potentials. A vector exchange gives rise to  $V_2$ ,  $V_3$  and  $V_4$ , a scalar exchange only to  $V_1$  (Gromes (1988)). In both cases, a constant term  $\sigma$  appears in  $V_2' - V_1'$  from the Gromes relation.

A useful quantity to study in this respect is the ratio of  $p$  state splittings:

$$\rho = \frac{M(^3P_2) - M(^3P_1)}{M(^3P_1) - M(^3P_0)}. \quad (37)$$

Experimentally this ratio takes the value 0.48(1) for  $c\bar{c}(1P)$  and 0.66(2) for  $b\bar{b}(1P)$  and 0.58(3) for  $b\bar{b}(2P)$ . For pure  $\mathbf{L} \cdot \mathbf{S}$  interactions  $\rho$  is simply related to a combination of expectation values of  $\mathbf{L} \cdot \mathbf{S}$  since, considering the spin-dependent potentials as a perturbation on the spin-independent one, the expectation value of  $V_i$  in all the  $P$  states is the same. This then gives  $\rho = 2$ . Similarly a pure tensor  $V_3$  interaction gives  $\rho = -0.4$ . These are clearly wrong; we require a mixture of spin-orbit and tensor terms. For the leading order perturbative potentials in equation 32 we can also calculate  $\rho$  exactly because all the expectation values of  $V_i$  reduce to cancelling terms of the form  $\langle r^{-3} \rangle$ . This gives  $\rho = 0.8$ , larger than all the experimental values. The confining term should then appear in such a way as to reduce  $\rho$ .

This is possible if we make the assumption that the confining term grows linearly with  $r$  as  $\sigma r$ ; such a rapid rise implies a scalar exchange (Gromes (1988)).  $V_1 = -\sigma r$  and  $V_2 = -C_F \alpha_s / r$  will satisfy the Gromes relation.  $\rho$  becomes

$$\rho = \frac{1}{5} \frac{8\alpha_s \langle r^{-3} \rangle - 5/2\sigma \langle r^{-1} \rangle}{2\alpha_s \langle r^{-3} \rangle - 1/4\sigma \langle r^{-1} \rangle} \quad (38)$$

and for positive expectation values this will be less than 0.8, in agreement with experiment (Henriques, Kellett and Moorhouse (1976)). The  $\sigma$  term will be more effective for longer range wavefunctions such as  $c\bar{c}$  and  $b\bar{b}(2P)$  giving a smaller value of  $\rho$  than for  $b\bar{b}(1P)$ . A vector confining potential would lead to the term proportional to  $\sigma$  appearing in  $V_2$  with opposite sign as well as additional  $V_3$  terms, so that  $\rho > 0.8$  (Schnitzer (1975)). Of course this does not rule out a mixture of long-range vector and scalar pieces.

The lattice calculation of the spin-dependent potentials confirm the behaviour above explicitly, and show (within errors) that the long range confining potential is purely scalar (Huntley and Michael (1987)).  $V_3$  and  $V_4$  are found to be very short-range with  $V_3$  showing  $1/R^3$  behaviour and  $V_4$  approximating a  $\delta$  function on the lattice.  $V_1'$  is approximately constant at the value  $-\sigma$  taken from the central potential, whereas  $V_2' \rightarrow 0$  at large  $R$ . In addition  $V_1'$  has a small attractive  $1/R^2$  piece (see Figure 12 from Bali, Schilling and Wachter (1997a)), which arises from the mixing between  $V_1$  and  $V_2$  and its size changes as the lattice cut-off ( $1/a$ ) changes, along with the Coulombic  $1/R^2$  term present in  $V_2'$ .

There is no exact Gromes relation on the lattice (Bali, Schilling and Wachter (1997b)), but it should be restored in the continuum limit. This relation does

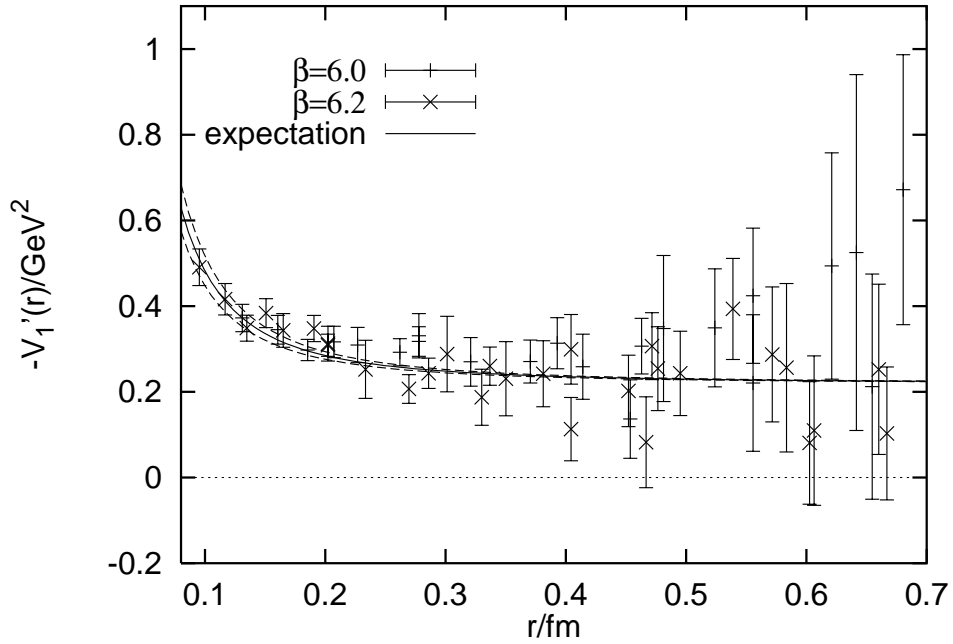


**Fig. 12.** The spin-orbit potential,  $-V_1'$ , at two different values of the lattice spacing together with a fit curve of the form  $\sigma + h/R^2$ . (Bali, Schilling and Wachter (1997a)).

in fact work well on the lattice at current values of the lattice spacing and this is a non-trivial check of the lattice renormalisation procedure of Figure 11 (Huntley and Michael (1987)). This renormalisation is done for the left hand side of equation 34 but not for the right. See Figure 13 from Bali, Schilling and Wachter (1997a).

As discussed earlier, the spectrum from this lattice potential yields deviations at the 10 MeV level for bottomonium and the 20 MeV level for charmonium. Systematic errors in the charmonium case are rather larger than this, however. The  $d_i$  coefficients have large perturbative corrections for the lattice cut-off used ( $m_c a < 1$ ) and so large uncertainties.  $c_1$  is set to 1 in equation 24; unknown perturbative corrections to that coefficient could induce 50MeV shifts in the charmonium spectrum (Bali, Schilling and Wachter (1997a)). As mentioned in section 2.1 there are also relativistic corrections to the spin-independent central potential (Barchielli, Brambilla and Prosperi (1990)). These can be calculated from expectation values of Wilson loops with  $E$  and  $B$  insertions in a similar way to that for the spin-dependent potentials above. The results modify the central potential for charmonium quite strongly, again indicating that unknown higher order corrections could be significant for that system.

To go beyond the corrections discussed here in the potential model approach

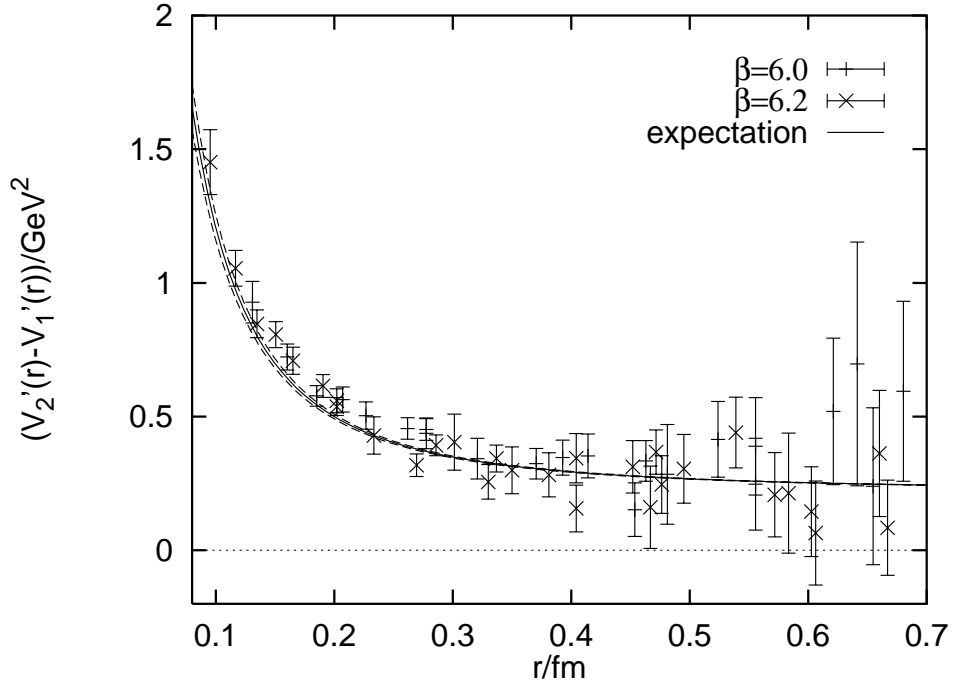


**Fig. 13.** The difference of spin-orbit potentials,  $V_2'$  and  $V_1'$  on the lattice, compared to the expectation from the central potential according to the Gromes relation. (Bali, Schilling and Wachter (1997a)).

is hard; higher order insertions into Wilson loops cannot be reduced to the form of an instantaneous potential. We need instead more direct methods of calculating the spectrum. This must be done on the lattice and will be discussed in the next subsection.

**Exercise:** Fill out Table 2 to include  $D$  states.

### 2.3 Direct measurement of the bottomonium spectrum on the lattice

A direct calculation of the heavyonium spectrum on the lattice at first sight seems rather hard. There is a large range of scales in the problem, all the way from the heavy quark mass to kinetic energies within bound states ( $\approx \Lambda_{QCD}$ ). To cover these properly in a lattice simulation would require  $a^{-1} \gg m_Q$  and the number of lattice points on a side,  $L \gg m_Q/\Lambda_{QCD}$ .

As we have seen from the previous sections, however, the quark mass itself is not a dynamical scale, simply an overall energy shift. We only actually need to simulate accurately the important scales for the bound state splittings,  $p_Q$



and  $K$ . This leads us to work with a lattice with  $a^{-1} < \mathcal{O}(m_Q)$  and make use of the non-relativistic effective theory of equation 22. This Lagrangian can be discretised on the lattice (Thacker and Lepage (1991), Lepage *et al* (1992)) and applied using similar techniques to those for handling light quarks on the lattice (Weingarten (1997), Montvay and Münster (1994)). Details will be discussed below.

There is an important difference between the NRQCD approach and the potential model approach of the section 2.2. That approach starts from the static theory and so can only produce the potential; the missing kinetic energy terms are of equal weight (in powers of  $v^2/c^2$ ) in the spectrum and they must be added in subsequently in a Schrödinger equation. The NRQCD calculations, even at lowest order, include both the  $\psi^\dagger D_t \psi$  term and the  $\psi^\dagger D^2/2m_Q \psi$  terms and yield the spectrum directly; the existence of a potential is not invoked at any stage. This means that the NRQCD approach can be fully matched to QCD and handle the sub-leading effects from soft-gluon radiation that eventually cause a potential model picture to break down through infra-red (long time) divergences (Appelquist *et al* (1978), Thacker and Lepage (1991)). We will find potential models useful for guiding NRQCD calculations, nevertheless.

The NRQCD approach uses the Lagrangian of equation 22 as an effective theory on the lattice (Lepage *et al* (1992)). It can reproduce the low energy ( $p < 1/a$ ) behaviour of QCD, but the couplings,  $c_i$ , must be adjusted from their tree level values of 1 to compensate for neglected high momentum interactions. In principle this can be done in perturbation theory by matching scattering amplitudes between lattice NRQCD and full QCD in the continuum (here a one-stage matching is used). The  $c_i$  will have an expansion in terms of  $\alpha_s(1/a)$ . They will differ from the  $c_i$  of the static approach discussed earlier since the  $\mathbf{p}^2/m_Q$  term in the heavy quark propagator will give additional explicit  $1/m_Q a$  terms which diverge as  $a \rightarrow 0$ . In this way it is clear that we cannot take a continuum limit in NRQCD; we can only demonstrate that results are independent of the lattice spacing at non-zero lattice spacing. This is sufficient for them to make physical sense, and to be compared to experiment.

One problem for lattice NRQCD is the possible large renormalisations,  $c_i$ , which come from tadpole diagrams. This was discussed earlier in connection with the renormalisation of the spin-dependent potentials in the static case. The tadpoles appear with every occurrence of a gluon link field and can be taken care of by renormalising each gauge link by a factor  $u_0$  as it is read in,

$$U_\mu \rightarrow \frac{U_\mu}{u_0}, \quad (39)$$

and then using the the renormalised gauge link everywhere instead of the original.

$u_0$  represents how far the gluon links are from their continuum expectation value of 1. The easiest quantity to use to set  $u_0$  is the plaquette. Since it contains four links we have:

$$u_0 = u_{0P} = \sqrt[4]{\frac{1}{3} \text{Tr} \langle \square \rangle} \quad (40)$$

A possibly better motivated value is that in which we look at a single link field and maximise its value by gauge-fixing. This should be most effective at isolating (by minimising) the true gauge-independent tadpole contribution (Lepage (1997)). The gauge in which this happens is Landau gauge:

$$u_0 = u_{0L} = \frac{1}{3} \text{Tr} \langle U_\mu \rangle_{\text{Landau gauge}}. \quad (41)$$

The difference between the two  $u_0$ s is small in lattice perturbation theory. Measured (non-perturbative) values on the lattice differ by a few percent at moderate values of the lattice spacing.

Once we have renormalised the gauge fields to take account of the tadpole contributions ('tadpole-improvement') we would hope that remaining corrections to the  $c_i$  are small. They have been calculated in perturbation theory for those terms which contribute to the heavy quark self-energy (Morningstar (1994)). The dispersion relation for the heavy quark is required to be

$$E(p) = \alpha_s A + \frac{p^2}{2m_r} - \frac{p^4}{8m_r^3} \quad (42)$$

with  $A$  an energy shift and  $m_r$  the renormalised quark mass, and this fixes the coefficient  $c_1$  in the lattice discretised version of equation 22. Figure 14 shows that the  $\mathcal{O}(\alpha_s)$  coefficient of  $c_1$  is small, its magnitude less than 1, until  $m_Q a$  is less than about 0.8, when it starts to diverge. This is a sign of the power ultra-violet divergences of NRQCD mentioned above; we must stay at values of  $a$  where  $m_Q a > 0.8$ . Without tadpole-improvement the  $\mathcal{O}(\alpha_s)$  coefficients are all much larger than 1 (Morningstar (1994)), showing that tadpole-improvement has captured most of the renormalisation. The results I shall describe here use tadpole-improvement and all  $c_i$  then set to 1.

The NRQCD Lagrangian is discretised on the lattice in the standard way (Weingarten (1997), Montvay and Münster (1994)). Derivatives are replaced by finite differences, and  $E$  and  $B$  fields by clover terms. In the process, all appearances of  $m_Q$  are replaced by the bare quark mass in lattice units,  $m_Q a$ , and powers of  $g$  are absorbed into the lattice fields. The lowest order terms in the Lagrangian density (in lattice units) become

$$D_t \psi_t \rightarrow U_t \psi_{t+1} - \psi_t \quad (43)$$

$$\frac{\mathbf{D}^2}{2m_Q} \rightarrow \frac{\sum_i U_{x,i} \psi_{x+\hat{i}} + U_{x-\hat{i},i}^\dagger \psi_{x-\hat{i}} - 2}{2m_Q a}.$$

Each  $U_\mu$  field here is understood to have been divided by  $u_0$  already.

Then the calculation of the heavy quark propagator is very simple. The propagator as a function of spatial indices on a given time slice is related to that on previous time slice by an evolution equation :

$$U_t G_{t+1} - G_t = -a H G_t \quad (44)$$

$$G_{t+1} = U_t^\dagger (1 - a H) G_t$$

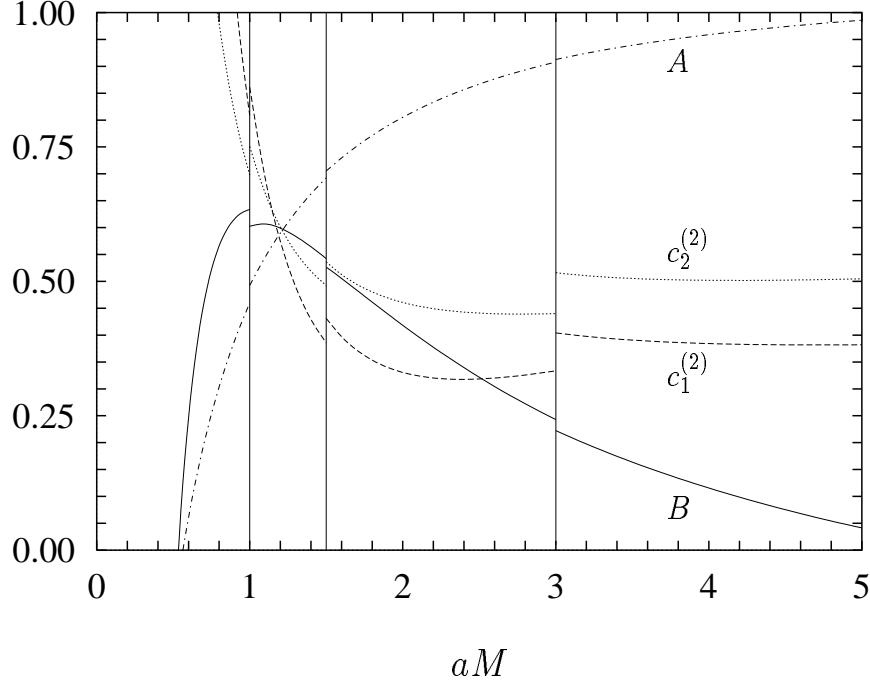


**Fig. 14.** The  $\mathcal{O}(\alpha_s)$  coefficients of various terms in the NRQCD Lagrangian, calculated in lattice perturbation theory *after* tadpole improvement.  $A$  corresponds to the energy shift and  $c_1^{(2)}$  to the  $D^4$  term.  $B$  corresponds to the mass renormalisation and  $c_2^{(2)}$  to the  $D_i^4$  term, here denoted  $c_5$ . The vertical lines represent discontinuities when the value of the stability parameter,  $n$ , is changed. (Morningstar (1994)).

where  $aH$  is the Hamiltonian, for example, the lowest order  $\mathbf{D}^2/2m_Q$  term, discretised on the lattice as in equation 43. This enables the heavy quark propagator to be calculated on one pass through the lattice in the time direction starting with some source for the propagator on time slice 1. This simplicity can be traced back to the simple first order time derivative in equation 22; calculations of relativistic quark propagators take many sweeps through the lattice (Weingarten (1997), Montvay and Münster (1994)).

One technical problem with (44) is that it can become unstable for modes for which  $H$  approaches 1. In the free case for the lowest order Hamiltonian we have

$$H_0 = \frac{3 \sum_i 4 \sin^2(p_i a/2)}{2m_Q a} \quad (45)$$

where  $i$  runs over the Fourier modes and the maximum value for momenta close to the lattice cut-off is  $6/m_Q a$ . This would limit values of  $m_Q a$  to be greater than

6. Instead we can stabilise the evolution by adding terms which have an effect at the cut-off scale but are not important for the physically relevant momenta well below the cut-off. This gives rise to an evolution equation (Thacker and Lepage (1991)):

$$G_{t+1} = \left(1 - \frac{aH}{2n}\right)^n U_t^\dagger \left(1 - \frac{aH}{2n}\right)^n G_t \quad (46)$$

and the stability requirement is now  $m_Q a > 3/n$  so reasonable values of  $m_Q a$  of  $\mathcal{O}(1)$  can be reached for suitable  $n$ . In fact it is only important to stabilise the lowest order term  $H_0$  like this; the higher order terms of the Lagrangian of equation 22 can be added in straightforwardly. For example, we can write (Lepage *et al* (1992)):

$$G_{t+1} = \left(1 - \frac{a\delta H}{2}\right) \left(1 - \frac{aH_0}{2n}\right)^n U_t^\dagger \left(1 - \frac{aH_0}{2n}\right)^n \left(1 - \frac{a\delta H}{2}\right) G_t \quad (47)$$

with  $a\delta H$  the lattice discretisation of :

$$\delta H = -c_1 \frac{(\mathbf{D}^2)^2}{8m_Q^3} + c_2 \frac{ig}{8m_Q^2} (\mathbf{D} \cdot \mathbf{E} - \mathbf{E} \cdot \mathbf{D}) - c_3 \frac{g}{8m_Q^2} \boldsymbol{\sigma} \cdot (\mathbf{D} \times \mathbf{E} - \mathbf{E} \times \mathbf{D}) - c_4 \frac{g}{2m_Q} \boldsymbol{\sigma} \cdot \mathbf{B}. \quad (48)$$

Another technical problem which faces all lattice calculations is that of discretisation errors. These arise from the use of finite differences on the lattice to approximate continuum derivatives. They mean that even physical lattice results, expressed in GeV for example, will depend upon the lattice spacing. The dependence will be as some power of a typical momentum scale in lattice units. Since the momenta inside heavyonium systems are quite large,  $\mathcal{O}(1 \text{ GeV})$ , discretisation errors will cause a problem if they are not corrected for.

This is achieved by improving the discretisation of derivatives to include higher order terms. For example, ignoring gauge fields,

$$\begin{aligned} a^2 D_{i,latt}^2 \psi_x &= \psi_{x+\hat{i}} + \psi_{x-\hat{i}} - 2\psi_x \\ &= (e^{aD_{i,cont}} - 1) (1 - e^{-aD_{i,cont}}) \psi_x \\ &= \left( a^2 D_{i,cont}^2 + a^4 D_{i,cont}^4 \left[ \frac{2}{6} - \frac{1}{4} \right] \dots \right) \psi_x. \end{aligned} \quad (49)$$

giving  $\mathcal{O}(a^2)$  errors relative to the leading term. A better discretisation is then

$$a^2 \tilde{D}_{i,latt}^2 = a^2 D_{i,latt}^2 - \frac{1}{12} a^4 D_{i,latt}^4 \quad (50)$$

where  $a^2 D_{i,latt}^2$  is given by the naïve finite difference.  $a^2 \tilde{D}_{i,latt}^2$  has errors at relative  $\mathcal{O}(a^4)$ .

The other operator that appears in the leading order terms is the time derivative operator,  $D_t$ . Any correction to  $D_t$  that looks like  $D_t^2$  would upset our simple evolution equation. Instead the way to correct  $D_t$  is to require that the time-step operator be

$$G_{t+1} = e^{-aH} G_t. \quad (51)$$

In fact the modified evolution equation (46) is closer to this than (44), and would be correct for the kinetic terms in the  $n \rightarrow \infty$  limit. The gauge potential will appear automatically exponentiated from the appearance of  $U_t^\dagger$ . The only correction that then needs to be made at the next order is to correct for a  $H_0^2/n$  term that appears when (46) is expanded out and compared to (51) for  $H = H_0$ . This correction can be made by replacing  $H_0$  by

$$\tilde{H}_0 = H_0 - \frac{aH_0^2}{4n}. \quad (52)$$

The discretisation corrections discussed here, when added in to  $\delta H$  look a lot like relativistic corrections. We can apply the same power counting arguments as before to get an idea of their relative size. From (52) we will have a correction of  $\mathcal{O}(am_Q^2 v^4)$ . Relative to  $H_0$  this is  $\mathcal{O}(am_Q v^2)$ , and for  $am_Q \sim 1$  this is  $\mathcal{O}(v^2)$ , the same as the relativistic corrections. Similarly for the term from (50). Thus it is only sensible to correct for the discretisation corrections up to an order comparable with the order of relativistic corrections being included. For the Lagrangian of 22 which has the first spin-independent relativistic corrections we need only the first spin-independent discretisation corrections described above. It might be true on coarse lattices, with  $m_Q a > 1$ , that higher order discretisation corrections should be kept. This can be decided by using potential model expectation values to better estimate their size (Lepage (1992)).

There are additional  $\mathcal{O}(a^2)$  errors from the gluon fields that appear in all the covariant derivatives coupling to the heavy quarks, if the gluon fields have been generated using the standard Wilson gluon action (Weingarten (1997), Montvay and Münster (1994)). These errors can be treated perturbatively and corrected for at the end of the calculation provided they are small (Davies *et al* (1995a)).

The coefficients of the additional terms introduced by the discretisation corrections in (50) and (52) must again be matched to full QCD. As before, they should be tadpole-improved to remove the largest part of the renormalisation of lattice NRQCD, and remaining renormalisations can be calculated in lattice perturbation theory. The improvement from (52) can be added directly to the existing relativistic correction to give the operator

$$\delta H_1 = c_1 \frac{a^4 (\mathbf{D}^2)^2}{8m_Q^3 a^3} \left(1 + \frac{m_Q a}{2n}\right). \quad (53)$$

The  $\mathcal{O}(\alpha_s)$  corrections to  $c_1$  were discussed above and are shown in Figure 14. The improvement from (50) gives

$$\delta H_5 = c_5 \frac{\sum_i a^4 D_i^4}{24m_Q a}. \quad (54)$$

The  $\mathcal{O}(\alpha_s)$  corrections to  $c_5$  are also shown in Figure 14 and they are confirmed to be small after tadpole-improvement (see Morningstar (1994) and note that  $c_5$  is there called  $c_2$ ).

Once the lattice NRQCD Lagrangian (including discretisation corrections) has been chosen and the quark propagator  $G_t$  calculated for a given gluon field configuration, then  $G_t$  and the anti-quark propagator  $G_t^\dagger$  can be put together to make mesons. This procedure is identical to that used in lattice calculations of the light hadron spectrum. The only difference is that the meson operator :

$$\psi^{\dagger A}(\mathbf{x}_1)\Omega\phi(\mathbf{x}_1 - \mathbf{x}_2)\chi^{\dagger A}(\mathbf{x}_2) \quad (55)$$

has a spin part,  $\Omega$ , which is only a  $2 \times 2$  matrix, rather than the relativistic  $4 \times 4$ .  $\Omega$  is the unit matrix for  $S = 0$  mesons and a Pauli matrix for  $S = 1$ . In addition we have a much better idea from potential models of what form the spatial operator should take, than we do in light hadron calculations. This will be discussed below.  $\psi^\dagger$  and  $\chi^\dagger$  are the quark and anti-quark creation operators respectively, matched in colour, denoted  $A$ , for a colour singlet.

Then the meson correlation function is calculated as an average over the ensemble of gluon field configurations (Weingarten (1997), Montvay and Münster (1994)):

$$\langle(\chi\phi^\dagger\Omega^\dagger\psi)_T(\psi^\dagger\Omega\phi\chi^\dagger)_0\rangle = \langle Tr[G\Omega^\dagger\phi^\dagger G^\dagger\phi\Omega]\rangle \quad (56)$$

$$\xrightarrow{T \rightarrow \infty} \Phi_1 e^{-E_1 T} + \Phi_2 e^{-E_2 T} + \dots$$

$E_1$  and  $E_2$  are the energies of states in lattice units,  $E_{\text{phys}a}$ .  $E_1$  is the energy of the ground state in that  $\Omega, \phi$  channel, and  $E_2$  is the energy of the first radial excitation etc. We can project onto different meson momenta at the annihilation time point,  $T$ , to obtain the dispersion relation,  $E$  as a function of  $p$  (Davies *et al* (1994a)).

Because it is very important in heavyonium physics to calculate radial excitation energies, we need to optimise the calculation of  $E_1$  and  $E_2$ . The coefficients  $\Phi_1$  and  $\Phi_2$  in (56) represent the overlap of the mesonic operator used with that state,  $\Phi_i = \langle 0|\psi^\dagger\Omega\phi\chi^\dagger|i\rangle$ , see equation 18. We can then adjust  $\Phi_1$  and  $\Phi_2$  by changing  $\phi$  in the mesonic operator. For  $S$  states we could use an operator in which both  $\psi$  and  $\chi$  appear at the same point but this would have overlap with all possible excitations and a poor convergence to the ground state. Instead we must  $\psi$  and  $\chi$  at separated points with  $\phi$  a ‘smearing function’. Potential model wavefunctions represent a good first approximation to the spatial distribution of quark and anti-quark in heavyonium (Davies *et al* (1994a)). To make use of these wavefunctions on the lattice (specifically to set  $\phi$  equal to the wavefunction) requires us to fix a gauge otherwise the meson operator will not be gauge-invariant and will vanish in the ensemble average. The best gauge to use is Coulomb gauge since this (being the 3-dimensional version of the lattice Landau gauge discussed earlier) is the gauge in which the spatial gluon field is minimised, and the covariant squared spatial derivative most like the Schrödinger  $\mathbf{p}^2$ . We then gauge transform the lattice gluon fields to Coulomb gauge and use different  $\phi$  as simple functions of spatial separation for different radial and orbital excitations. For the ground state  $\phi$  should maximise  $\Phi_1$  and minimise  $\Phi_2, \Phi_3$  etc, and for excited states  $\phi$  should maximise  $\Phi_2$  and minimise  $\Phi_1, \Phi_3$  etc. For each  $\phi$  a new quark

propagator must be calculated in this approach since the fastest way to make the meson operator at the initial time slice is to use  $\phi(\mathbf{x})$  as a source for the evolution equation for  $G_t$ . This  $G_t$  is then combined with a  $G_t^\dagger$  in which a delta function at the spatial origin was used as the source. The same source  $\phi$  can be used for the different spin states (to the extent that spin-dependent effects on the wavefunction are relativistic corrections and therefore small) and the factors of  $\Omega$  at the initial time slice inserted as  $G_t$  and  $G_t^\dagger$  are being combined. In this way all  $^{2S+1}L_J$  states can be made with as many radial excitations as required (Davies *et al* (1994a)).

It is important to realise that the results for  $E_1$  and  $E_2$  are not affected by the choice of  $\phi$ ; they can simply be obtained more efficiently by good choices. Methods other than that above have also been used; these include building meson operators out of a quark and anti-quark joined by a string of gauge fields in a gauge-invariant way (Manke *et al* (1997)); and calculating the propagators from delta function sources at a number of spatial points at the initial time and working out the optimal  $\phi$  at the end using a variational method (Draper *et al* (1995)).

However good the choice of  $\phi$ , each meson correlation function will contain several exponentials and a multi-exponential fit must be performed to extract them. This is described with technical details in Davies *et al* (1994a). In general the  $n$ th exponential is obtained reliably from an  $n + 1$ -exponential fit. In a potential model approach to the spectrum, using orthogonal wavefunctions, it is easy to get very precise results for radially excited states. In lattice NRQCD it is much harder because the ground state will take over exponentially if it is present at all in an excited meson correlation function. In addition the variance of such a correlation function will be dominated by the ground state so that the ratio of the signal for the excited state compared to noise will fall exponentially (see, for example Lepage (1989)).

The fits to the zero momentum meson correlation functions yield a very accurate set of energies in lattice units but these cannot be immediately converted to absolute energies (although splittings can) because the zero of energy has been reset by the absence of the mass term in equation 22. To calculate the spectrum we must shift all the lattice energies by a constant and then convert to physical units by multiplication with  $a^{-1}$ .

Determining the lattice spacing is actually easier in heavyonium than for light hadrons. We can make use of the fact, stated before, that the radial and orbital splittings are independent to a very good approximation of the heavy quark mass. This means that we can use one of these splittings, e.g. the  $1\bar{P} - 1\bar{S}$  splitting, to determine  $a^{-1}$ , without having necessarily tuned our heavy quark mass very well. In the absence of an experimentally determined spin-average  $S$  state mass for bottomonium we set

$$a^{-1} = \frac{0.44}{aE(\bar{\chi}\bar{b}) - aE(\Upsilon)} \text{GeV}. \quad (57)$$

where the denominator is the difference between the lattice energies at zero

momentum of the spin average of the ground  $\chi_b$  states and the  $\Upsilon$ . Given  $a^{-1}$  we can now convert all differences in energy to splittings to GeV. We can also use  $E(\Upsilon') - E(\Upsilon)$  to set  $a^{-1}$ .

To tune the bare lattice heavy quark mass,  $m_Q$ , to the appropriate value for the  $b$  quark we study the dispersion relation for mesons at finite and small momenta, where the heavy mesons are non-relativistic. The absolute meson mass (e.g. for the  $\Upsilon$ ) is given not by the energy at zero momentum but by the denominator of the kinetic energy term :

$$aE_{\Upsilon}(p) = aE_{\Upsilon}(0) + \frac{a^2 p^2}{2aM_{\Upsilon}} + \dots \quad (58)$$

Higher order relativistic corrections can also be added to this formula. We adjust  $m_Q a$  in the Lagrangian until the  $\Upsilon$  mass comes out at 9.46 GeV within statistical errors, using the  $a^{-1}$  determined from the splitting above. Now it is clear that if the splittings used for determining  $a^{-1}$  did depend strongly on  $m_Q a$  this would be a tricky iterative procedure. It would require complete calculations at several different values of  $m_Q a$ , as is generally undertaken in light hadron calculations.

This procedure gives us also the shift of the zero of energy,  $aM_{\Upsilon} - aE_{\Upsilon}(0)$ . It should be independent of the meson studied and so, once calculated, can be applied to all mesons. That is, when divided by 2, it can be applied as a shift per quark. This is what allows us to convert differences in zero momentum energies on the lattice directly to splittings in physical units, given  $a^{-1}$ .

The shift obtained can be compared to that calculated in lattice perturbation theory from the heavy quark self-energy. The energy shift is given in lattice units by

$$2(Z_m m_Q a - E_0 a) \quad (59)$$

where  $Z_m$  is the mass renormalisation.  $Z_m$  and  $E_0 a$  are given by perturbative expansions,  $Z_m = 1 + \alpha_s B + \dots$  and  $E_0 a = \alpha_s A + \dots$ . Again it is clear that  $A$  and  $B$  are smaller when a tadpole-improved lattice Lagrangian is used. (see Morningstar (1994) and Figure 14). The shifts obtained on the lattice agree well with the perturbative estimates (Davies *et al* (1994a), Davies (1997)) when a physical scheme for the lattice coupling constant is used (Lepage and Mackenzie (1993)) and allowance is made for unknown higher order terms. See Table 3.

Note that if we take  $m_Q a$  to  $\infty$  in this calculation  $aE_0$  will become  $V_c/2$  where  $V_c$  is the unphysical self-energy part of the heavy quark potential discussed earlier. Again agreement between perturbation theory (Morningstar (1994), Duncan *et al* (1995)) and potential model results (Bali and Schilling (1992)) is reasonable given that  $aE_0$  starts at  $\mathcal{O}(\alpha_s)$  and is only known to this order. The effect of tadpole-improvement is easy to work out in this case. If the Wilson loops were calculated with tadpole-improvement (not usually done) then each  $U_{\mu}$  would be divided by  $u_0$  and the loop would pick up a factor  $(u_0)^{-2T}$  from links in the time direction. Then  $V_c \rightarrow V_c + 2 \ln u_0$ . Thus to compare the perturbative value of  $aE_0(m_Q a \rightarrow \infty)$  calculated *with* tadpole-improvement to the non-perturbative values of  $V_c/2$  calculated *without* tadpole-improvement we must subtract  $\ln u_0$



$\beta$	$m_Q a$	Perturbative shift	Non-perturbative shift
5.7	3.15	7.0(6)	6.54(7)
6.0	1.71	3.5(2)	3.49(3)
6.2	1.22	2.5(2)	2.58(3)

**Table 3.** Energy shifts for a heavy quark in lattice NRQCD. Results are given for the non-perturbative lattice calculation of  $aM_\Upsilon - aE_\Upsilon(0)$  and for the perturbative shift of equation 59 for three different values of the lattice spacing, set by  $\beta$ , and for bare quark masses appropriate to the  $b$ . Errors in the perturbative shifts are estimates of unknown higher order corrections. (Davies (1997)).

from the perturbative calculation. It is also true that  $B$  for  $m_Q a \rightarrow \infty$  vanishes at  $\mathcal{O}(\alpha_s)$  so  $Z_m \rightarrow 1$ . Since the dispersion relation for mesons at finite momentum cannot be obtained from potential model approaches, the quark mass there has to be fixed in a different way to the direct NRQCD method above. If the energies of states are calculated using the lattice potential including  $V_c$ ,  $m_Q a$  should be adjusted until experiment is matched for, say, the  $\Upsilon$  on applying a shift  $2m_Q a - V_c$  (Bali, Schilling and Wachter (1997a)).

Figures 15 and 16 show recent results for the bottomonium spectrum from lattice NRQCD. The errors shown on the plot are statistical errors only - it is clear that they are significantly smaller than those from light hadron calculations. The simple form of the evolution equation for calculating the heavy quark propagator means that an average over a very large ensemble of gluon fields can be obtained with moderate computing cost. Also several different starting points can be used on a single gluon field configuration.

The sources of systematic error are also under better control than for light hadron calculations. There, one of the most serious problems is that of finite volume. A large enough lattice is required not to squeeze the mesons under study and distort their masses. Because the  $\Upsilon$  is much smaller than, say, the  $\rho$ , a smaller space-time box is sufficient for its study. The calculations shown were done on lattices of around 1.5fm on a side. However, radial and orbital excitations are larger than ground states and such a lattice may be too small for  $3S$  and  $2P$  states. Studies on larger volumes should be done for these in future. In fact direct calculations of the spectrum have worse finite volume errors than calculations of the heavy quark potential, because of lattice symmetries that protect  $V(R)$  (Huntley and Michael (1986)).

Discretisation errors are an additional source of systematic error and in all the results shown, the leading discretisation corrections have been made as described above.

Since NRQCD is a non-relativistic expansion, there are systematic errors from higher order relativistic terms that have been neglected. For the spin-independent terms all groups have used the lattice-discretised version of the Lagrangian of equation 22. This includes leading terms of  $\mathcal{O}(m_Q v^2)$  and correc-

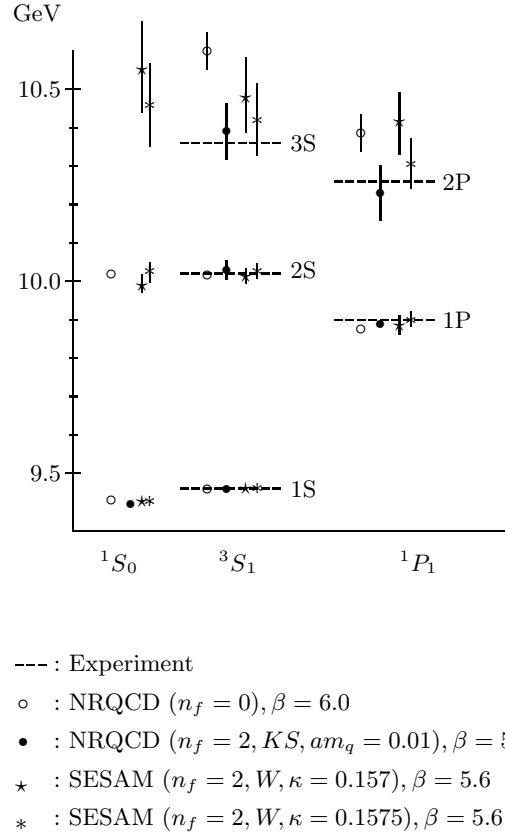


**Fig. 15.** Radial and orbital excitation energies in the  $\Upsilon$  spectrum from lattice NRQCD obtained by different groups (Davies *et al* (1997), SESAM (1997)). Errors shown are statistical only. The scale has been set by an average of  $a^{-1}$  from the  $2S - 1S$  splitting and that from the  $1P - 1S$ . Experimental results are given by dashed lines and for the  $1P_1$  state is taken as the spin-average of the  $\chi_b$  states.

tions of  $\mathcal{O}(m_Q v^4)$ . Errors are therefore at  $\mathcal{O}(m_Q v^6)$ , giving  $v^2 \times$  (a typical kinetic energy) =  $0.01 \times 400$  MeV for bottomonium =  $\sim 4$  MeV. This error would be invisible on Figure 15, since it is a 1% error in the splittings shown. For the spin-dependent terms a 4 MeV error is more significant since splittings are smaller. This is the error estimate if only the leading spin-dependent terms of equation 22 are used, as by the NRQCD collaboration (Davies *et al* (1994a)). The SESAM group (results presented at this school by Achim Spitz - see Spitz (1997) and SESAM (1997)) however has used the additional relativistic corrections to the spin-dependent terms given in the continuum by (Lepage *et al* (1992)):

$$\delta H = -c\tau \frac{g}{8m_Q^3} \{ \mathbf{D}^2, \boldsymbol{\sigma} \cdot \mathbf{B} \} \quad (60)$$

$$\begin{aligned}
 & -c_8 \frac{3g}{64m_Q^4} \{ \mathbf{D}^2, \boldsymbol{\sigma} \cdot (\mathbf{D} \times \mathbf{E} - \mathbf{E} \times \mathbf{D}) \} \\
 & -c_9 \frac{ig}{8m_Q^3} \boldsymbol{\sigma} \cdot \mathbf{E} \times \mathbf{E}.
 \end{aligned}$$

This could reduce the relativistic error by another factor of  $v^2$  to around 1% for spin splittings also. The SESAM group tadpole-improve all the terms above using  $u_{0L}$  and set the  $c_i$  to 1. In principal, however, unknown radiative corrections from lower order terms, e.g.  $\mathcal{O}(\alpha_s)$  corrections to  $c_4$  beyond tadpole-improvement, can produce errors at the same order as the terms of (60) (if we take  $\alpha_s \sim v^2 \sim 0.1$ , but see Bodwin *et al* (1995)) so this is not a complete calculation at the next order. Note that relativistic corrections to spin-dependent terms are not known for a potential model.

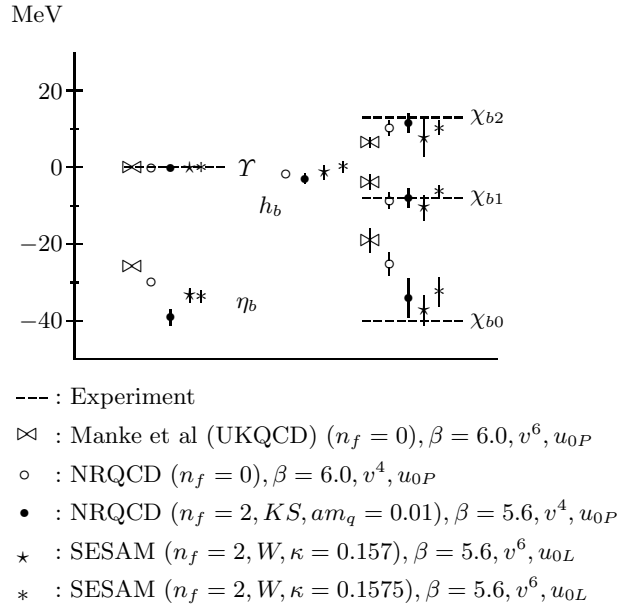


**Fig. 16.** Fine structure splittings in the ground state  $\Upsilon$  spectrum from lattice NRQCD obtained by different groups (Manke *et al* (1997), Davies *et al* (1997), SESAM (1997)). Errors shown are statistical only. The scale is set as in Figure 15. Experimental results are given by dashed lines. The spin-average of the  $\chi_b$  states has been set to zero.

Figure 15 compares radial and orbital splittings to experiment. The lattice spacing chosen to set the scale is an average of that from the  $1P - 1S$  splitting and that from the  $2S - 1S$  splitting. One striking feature is the disagreement with experiment for the calculation on quenched configurations ( $n_f = 0$ ). The results on the partially unquenched configurations ( $n_f = 2$ ) give much better

agreement. A quantity which exposes this error in the quenched approximation is the ratio of the  $2S-1S$  splitting to that of the  $1P-1S$ . Figure 17 demonstrates that the fact that this ratio is too large is a physical effect - it is not affected substantially by lattice discretisation errors. We expect such an effect in the quenched approximation because  $\alpha_s$  runs incorrectly between scales. This means, as discussed earlier, that the quenched heavy quark potential is too high at small values of  $R$  and so the  $S$  states are pushed up with respect to  $P$  states, making the  $1P-1S$  splitting too small relative to the  $2S-1S$ . The effect may be stronger for higher excitations, but they are subject to larger lattice errors.

The error from the quenched approximation is even bigger if we look at quantities sensitive to a larger disparity of scales to maximise the effect of incorrect running. Figure 18 shows the ratio of the  $1P-1S$  splitting in bottomonium from the NRQCD collaboration to the  $\rho$  mass from the UKQCD (UKQCD (1997)) and GF11 collaborations (Butler *et al* (1994), Weingarten (1997)). The UKQCD  $\rho$  mass results have included discretisation corrections for the light quarks; the GF11 results have not. It is clear that, although a result independent of lattice spacing is obtained when the  $\rho$  mass is improved, it is wrong.

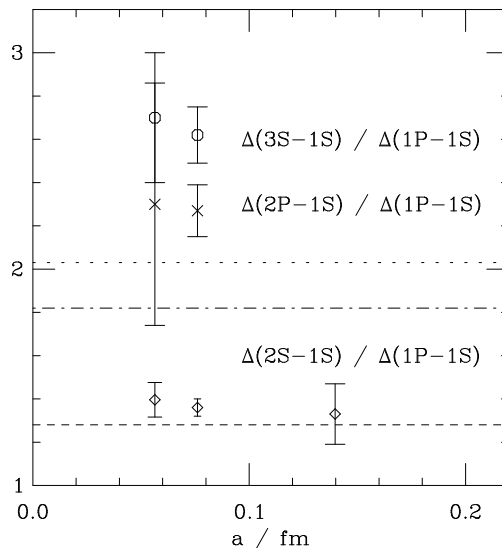


**Fig. 17.** Dimensionless ratios of various splittings to the  $\overline{\chi}_b - \Upsilon$  splitting against the lattice spacing in fm, set by the  $\overline{\chi}_b - \Upsilon$  splitting, in the quenched approximation. Experimental values are indicated by lines. (Davies (1997)).

The fine structure in the spectrum is shown in Figure 16. As already dis-

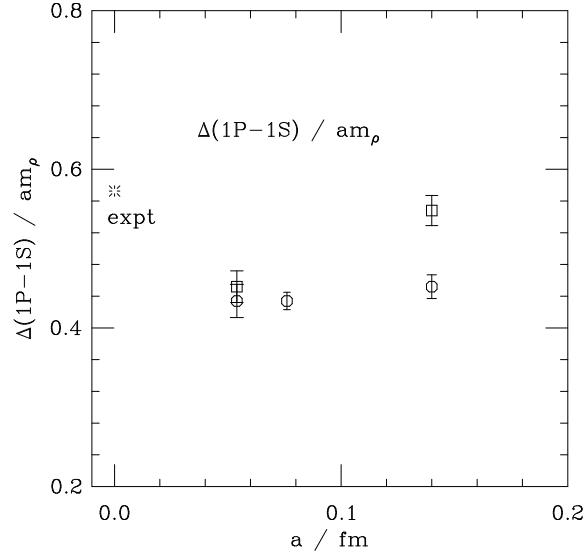


**Fig. 18.** Dimensionless ratio of the  $\bar{\chi}_b - \Upsilon$  splitting to the  $\rho$  mass against the lattice spacing in fm, set by the  $\bar{\chi}_b - \Upsilon$  splitting in the quenched approximation (Davies (1997)). Circles show the UKQCD improved  $\rho$  mass and the squares the GF11 unimproved mass. Experiment is shown by the burst.

cussed, this is harder to calculate accurately than the spin-independent spectrum because it only appears as a relativistic correction. There is no large leading order term with non-perturbatively determined coefficient to stabilise the results as there is in the spin-independent case ( $\mathbf{D}^2/2m_Q$ ). Since the clover discretisation of  $E$  and  $B$  fields each contain four links (see figure 10) there are several powers of  $u_0$  in each term when tadpole-improvement is undertaken. This means that spin-splittings are affected strongly by the value of  $u_0$  and if  $u_0$  were set to 1 (i.e. no tadpole-improvement) results much smaller than experiment would be obtained (Davies *et al* (1994a)). This also means that the spin splittings change when different definitions of  $u_0$  are used, in the absence of a perturbative calculation of the remaining radiative corrections (for preliminary results on these, see Trotter (1997b)). The difference between  $u_{0P}$  and  $u_{0L}$  results in 10-20% shifts to the splittings at these lattice spacings (SESAM (1997)). The hyperfine splitting is particularly sensitive; in leading order perturbation theory it is proportional to  $c_4^2$  (equivalent to  $u_0^{-6}$  when  $u_0$  factors in the  $\mathbf{D}^2$  term are taken into account). The presence or absence of the higher order relativistic corrections also affects the results at a similar level (Manke *et al* (1997), SESAM (1997)). Discretisation corrections, not surprisingly, are important as well. Because the fine structure (and particularly the hyperfine splitting) is sensitive to short-distance scales (consider

the functional form of the spin-dependent potentials), the discretisation errors can be quite severe. In the calculation of the NRQCD collaboration in which only leading order spin terms are included, the hyperfine splitting in MeV shows strong dependence on the lattice spacing - see Figure 19. This makes a physical result hard to determine. Results of the other groups in Figure 16 include, along with the relativistic spin-dependent corrections, discretisation corrections to the leading spin-dependent terms (Lepage *et al* (1992)). This should reduce the lattice spacing dependence of the physical results but this analysis is not yet complete (see Figure 19 and Manke (1997)). Finally the spin splittings depend quite strongly on the quark mass (particularly again the hyperfine splitting) and for these the quark mass must be tuned accurately. This requires a very accurate determination of the meson kinetic mass as well as of the lattice spacing.

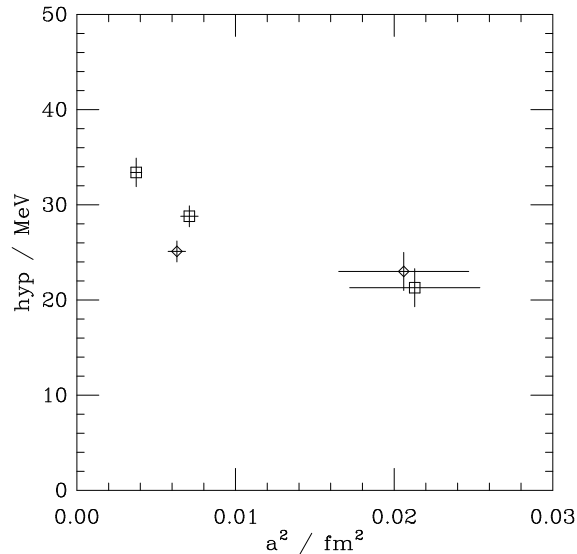


**Fig. 19.** The  $\Upsilon - \eta_b$  splitting in physical units vs the square of the lattice spacing in fm in the quenched approximation. The  $2S - 1S$  splitting has been used to set the scale. Squares are results from the lowest order action (Davies (1997)) and diamonds from an action which includes spin-dependent relativistic and discretisation corrections (Manke *et al* (1997), Manke (1997)).

To compare to the real world we would like results with dynamical fermions of appropriate number and mass. To estimate how many dynamical fermions are ‘seen’ by the bottomonium system, we need to know what the typical momenta being exchanged by the heavy quarks are. For  $\Upsilon$  this  $q_T$  is about 1 GeV, not

enough to make a  $c\bar{c}$  pair, so the effective value of  $n_f$  should be 3. Almost all available sets of gluon field configurations have  $n_f$  set to 2, so extrapolation is necessary. The results will also depend on the light quark mass of the dynamical flavours, and this dependence at worst should be linear (Grinstein and Rothstein (1996)):

$$\Delta M \sim \Delta M_0 \left( 1 + c \sum_{u,d,s} \frac{m_q}{q\bar{r}} \dots \right) \quad (61)$$

For  $q\bar{r} \gg m_q$  the answer with  $u, d$  and  $s$  quarks can be reproduced by 3 degenerate dynamical quark flavours of mass  $m_s/3$  (ignoring  $m_u$  and  $m_d$ ). Results should be extrapolated as a function of dynamical fermion mass to  $m_s/3$  and then extrapolated to  $n_f = 3$  from  $n_f = 0$  and 2.

In fact no significant  $m_Q$  dependence has been seen by the two groups, NRQCD and SESAM, who have done calculations on dynamical configurations (using different lattice formulations of the light fermions). The SESAM collaboration with 3 dynamical quark masses does see a definite trend in  $m_q$ , however (SESAM (1997)). Figure 20 shows the dependence of the ratio of the  $2S - 1S$  to  $1P - 1S$  splitting on  $n_f$  for the two groups. The results are consistent with experiment for  $n_f = 3$  but  $n_f = 2$  cannot be ruled out without better statistics. More points at other values of  $n_f$  would be useful.

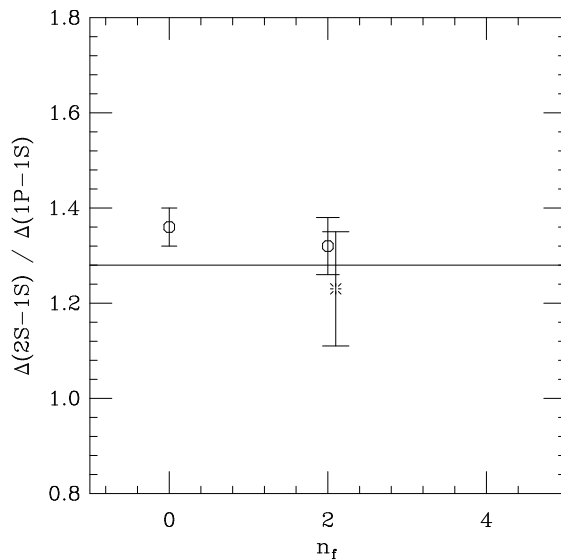


**Fig. 20.** The ratio of the  $\Upsilon' - \Upsilon$  splitting to the  $\bar{\chi}_b - \Upsilon$  splitting as a function of the number of dynamical flavours. Circles are the results from the NRQCD collaboration (Davies *et al* (1997)) and the burst from the SESAM collaboration (SESAM (1997)).

The  $n_f$  extrapolation of the fine structure will be more difficult, even once physical results at a given  $n_f$  are obtained. Since the fine structure probes much shorter distances it is possible that the effective number of flavours that it ‘sees’ is higher. Then the challenge will be to find appropriate quantities to set the scale for an extrapolation to, say,  $n_f = 4$ . It will not be possible to use spin-independent splittings for which the real world  $n_f$  value is 3 (Davies (1997)).

Figure 16 shows disagreement with experiment for the  $P$  fine structure in the quenched approximation, both in overall scale and for the ratio  $\rho$ , equation 37. Agreement is better on unquenched configurations, but the systematic errors described above must be removed before this is clear. The hyperfine splitting is very sensitive to the presence of dynamical fermions. It increases by  $\sim 30\%$  as  $n_f$  is increased from 0 to 2 for the NRQCD results (see Figure 16). Extrapolations in  $n_f$  using a variety of other short-distance quantities to set the scale (so the physical results differ from those in Figure 16) give a ‘real world’ value for the hyperfine splitting of around 40 MeV. The error is very large at present (25%) because of the inaccuracies in the fine structure. With improved calculations this can be reduced to 10%.

## 2.4 Direct measurement of the charmonium spectrum on the lattice

Unfortunately the NRQCD programme as described for bottomonium does not work as well for charmonium. It has been clear all along that charmonium is much more relativistic; with the NRQCD approach we can directly see the effects of higher order relativistic corrections to the Lagrangian. A calculation with the Lagrangian of equation 22 has errors at  $\mathcal{O}(m_Q v^6)$  as discussed earlier (Davies *et al* (1995b)). This gives an error of around 30MeV which is 30% for spin splittings. On adding higher order terms these large corrections to the fine structure become manifest (Trottier (1997a)) and are actually rather worse than the naive 30%. An accurate calculation of the  $\psi - \eta_c$  splitting, for example, would then require a high order in the NRQCD expansion, coupled with the determination of radiative corrections to the coefficients.

It seems more useful to treat the  $c$  quark as a light quark and use standard lattice approaches for relativistic quarks (Weingarten (1997), Montvay and Münster (1994)). However, the fact that  $m_{ca} \sim 1$  on current lattices can lead to significant discretisation errors. The heavy Wilson approach (El-Khadra *et al* (1997)) is an adaption of the standard Wilson light fermion action in which higher dimension operators are added to better match to continuum QCD by reducing errors of the form  $(p_Q a)^n$ . The coefficients of these operators must be calculated and in the strict heavy Wilson approach they are considered as a perturbative series in  $\alpha_s$  but to all orders in  $m_Q a$ . At large  $m_Q a$  the Lagrangian becomes NRQCD-like (since no symmetry between space and time directions is imposed) and at small  $m_Q a$  it reduces to the form used for the Symanzik improvement of light quarks. In principle it can span the region from one extreme to the other. In practise, NRQCD is rather simpler and faster to implement for really non-relativistic fermions.



The lowest order heavy Wilson action is identical to the Sheikholeslami-Wohlert (SW) action for light quarks in which a clover term

$$\frac{ig}{2}c_s w \kappa \bar{\psi}(x) \sigma_{\mu\nu} F^{\mu\nu} \psi(x) \quad (62)$$

with  $m_Q a$ -independent coefficient is added to the Wilson action (Sheikholeslami and Wohlert (1985), Heatlie *et al* (1991)):

$$S = \sum_n \bar{\psi}_n \psi_n - \kappa \sum_{n,\mu} [\bar{\psi}_n (1 - \gamma_\mu) U_{n,\mu} \psi_{n+\hat{\mu}} + \bar{\psi}_{n+\hat{\mu}} (1 + \gamma_\mu) U_{n,\mu}^\dagger \psi_n]. \quad (63)$$

The coefficient of the clover term is usually taken as 1 after the gauge fields have been tadpole-improved, and perturbative calculations to  $\mathcal{O}(\alpha_s)$  ( $m_Q a \rightarrow 0$ ) indicate no large additional radiative corrections (see Lüscher *et al* (1997) for a discussion). Non-perturbative determinations of this clover coefficient for the light quark case are described by Sommer (1997).

The meson energy-momentum relation must also be considered carefully for charm systems (El-Khadra *et al* (1997)). For the SW action there is an energy shift between the energy at zero momentum (the pole mass) and the kinetic meson mass that sits in the denominator of the kinetic term, as in the NRQCD case (equation 58). The shift increases as the quark mass increases and for  $m_Q a > 0.5$  it is important that the physical meson mass is taken from the kinetic mass and not from the pole mass which is used for light hadrons. It is possible to remove this shift by adjusting coefficients in the full heavy Wilson approach, but it is not necessary.

For the SW action there is also a problem with non-universality of the shift. It should appear simply as a shift per quark and therefore twice as big for a meson with two heavy quarks as for a meson with one heavy and one light quark. However there is a discrepancy between the shift per heavy quark in these two cases and it increases significantly as the heavy quark mass increases (Collins *et al* (1996a), Aoki *et al* (1997), see Figure 21). The discrepancy arises from lattice discretisation errors in relativistic  $\mathbf{D}^4$ -type terms in the heavy quark action affecting the heavy-heavy mesons. These terms need to be correct in order for the binding energy of a meson to be fed into its kinetic mass. Since the kinetic mass appears at  $\mathcal{O}(m_Q v^2)$  it is  $\mathcal{O}(m_Q v^4)$  terms which do this, whereas the pole mass is  $\mathcal{O}(1)$ . If the  $\mathcal{O}(m_Q v^4)$  terms are incorrect, the binding energy will appear only in the pole mass and the shift will then depend on the binding energy. For a heavy-light meson the binding energy is provided by the light quark and this problem does not arise. In the NRQCD case (Davies *et al* (1994b)) the relativistic terms are correct because the  $\mathbf{D}^4/8m_Q^3$  term is added by hand and discretisation corrections remove  $D_i^4$  rotational non-invariance. For the SW action this isn't true; the  $\mathbf{D}^4$  term has an incorrect mass and there is an uncancelled  $D_i^4$  term (Kronfeld (1997)). Both these effects can be corrected for in the heavy Wilson approach (El-Khadra *et al* (1997)), but this has not been done as yet. For charm quarks with  $m_c a < 0.5$  there is not a significant problem, as in clear from Figure 21.

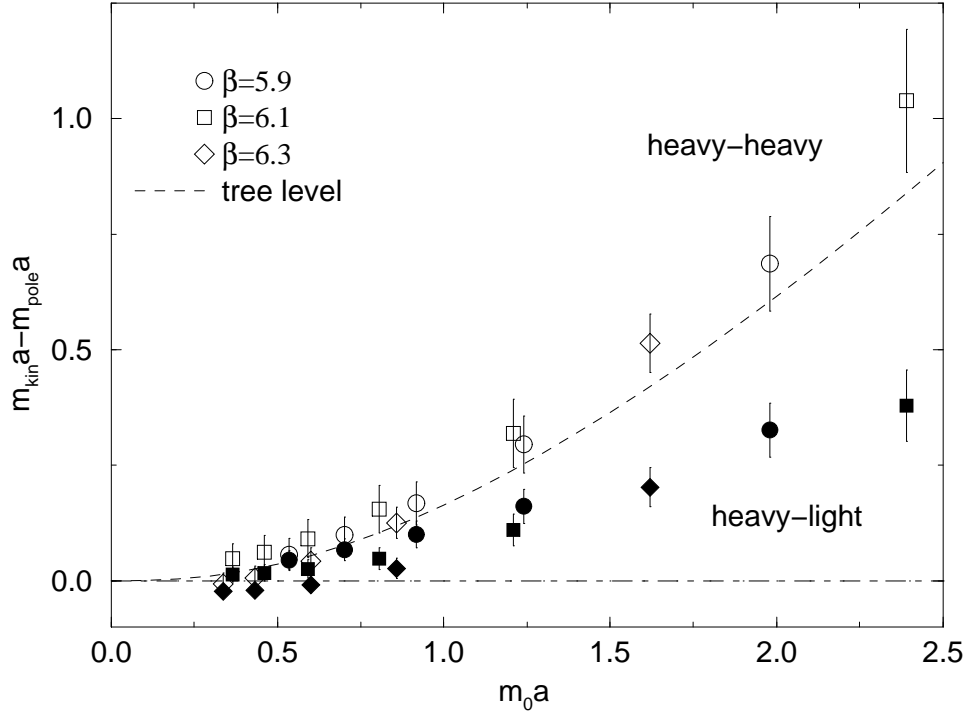


**Fig. 21.** The energy shift per heavy quark for the SW action, as a function of heavy quark mass,  $m_0 a$ . Note the difference between results for heavy-heavy mesons (open symbols) and those for heavy-light mesons (filled symbols). (Aoki *et al* (1997)).

The calculation of charm quark propagators with the SW action proceeds as for conventional light quarks (Weingarten (1997), Montvay and Münster (1994)) with the calculation of rows of the fermion matrix inverse by an iterative procedure. This converges quite rapidly for heavy quarks, but care must be taken to allow enough iterations for the solution to propagate over the whole lattice. Meson correlation functions are put together using various smearing functions and then fitted to multi-exponential forms as described for the NRQCD case. The charm quark mass is tuned by the kinetic mass method as before.

Figure 22 shows the spectrum for charmonium calculated recently on quenched gluon fields with this method and presented at this school by Peter Boyle (Boyle (1997b)). Previous results (El-Khadra and Mertens (1995)) are in agreement with this, but don't show such complete fine structure. The hyperfine splitting is clearly underestimated and this could be a quenching error, since this splitting increases with  $n_f$ , as discussed in the bottomonium case, or it could mean that  $c_s$  is underestimated. The fine structure also shows a discrepancy for the ratio  $\rho$

(see equation 37).

The systematic errors of the SW action for charmonium need some analysis (El-Khadra and Mertens (1995)) before we can extract physical (quenched) results from these calculations. Only one calculation on unquenched configurations has been done (Collins *et al* (1996a)) and problems with fitting errors made it hard to draw conclusions.

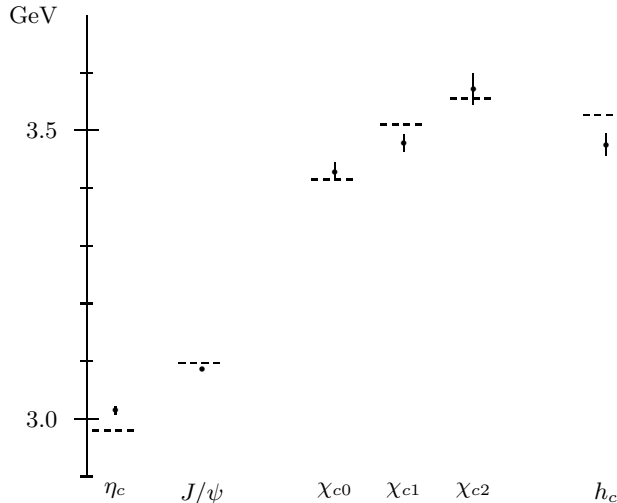


**Fig. 22.** The charmonium spectrum from quenched lattice QCD using the SW action (Boyle (1997b)).

Future work will need to investigate the use of actions with higher order terms, possibly on anisotropic lattices (Lepage (1996)). Some preliminary work on the charmonium spectrum has been done with these (Alford *et al* (1997)). A small lattice spacing in the time direction is useful for improving exponential fits, particularly for excited states, and does not need to mean a small lattice spacing in the spatial directions. Indeed such an anisotropy is very natural for non-relativistic systems, as we have seen.

## 2.5 Other heavy-heavy states

There is a lot of interest in the literature in other heavy-heavy bound states, which have not yet been seen experimentally. The one most likely to be seen in the near future is the mixed bound state of bottom and charm quarks; indeed candidates for the  $^1S_0$  ground state, the  $B_c$ , have been seen recently (DELPHI (1997a), ALEPH (1997)).

The  $b\bar{c}$  system actually has a lot in common with the heavy-light systems of the next section, although it is classified here as heavy-heavy because of its quark

content. The charm quark in the  $B_c$  will be more tightly bound and therefore more relativistic than in charmonium, and we have already seen that a non-relativistic approach to charmonium is rather inaccurate. In addition, because charge conjugation is not a good quantum number, the two  $1^+$   $P$  states will mix to give a different  $P$  fine structure to that for heavyonium.

Recent continuum potential model results for the  $b\bar{c}$  spectrum are given in Eichten and Quigg (1994) and Gershtein *et al* (1995). 2 sets of  $S$  states, 1 set of  $P$  states and 1 set of  $D$  states are expected below threshold for the Zweig allowed decay to  $B, D$  (7.14 GeV). Note that the  $b\bar{c}$  states below threshold are particularly stable since the annihilation mode to gluons is also forbidden.

First lattice calculations (Davies *et al* (1996)) have used NRQCD for both the  $c$  and  $b$  quarks. Agreement with potential model results was found within sizeable systematic uncertainties. Better calculations will use NRQCD for the  $b$  quark and relativistic formulations for the  $c$  quark (Shanahan (1997)). However, uncertainties still remain about how to fix the bare quark masses in the quenched approximation, because of the variations possible in the determination of the scale. These problems should become more tractable when complete calculations are done including the effects of dynamical fermions. Only preliminary results are available on unquenched configurations using NRQCD for  $b$  and  $c$  (Gorbahn *et al* (1997)). Figure 23 shows a comparison of the spectrum for lattice and potential model results.

Other states of a more speculative nature are hybrid states which include a gluonic valence component;  $Q\bar{Q}g$ . Observation of these states would be a direct confirmation of the non-Abelian nature of QCD (see possibly E852 (1997)). Hybrids are expected containing all quark flavours, but the advantage of studying the heavy-heavy hybrids is that the normal  $Q\bar{Q}$  spectrum is relatively clean, both experimentally and, as discussed here, theoretically.

There have been several lattice calculations of the hybrid potentials for a potential model analysis of these states (see, for example, Perantonis and Michael (1990), Juge, Kuti and Morningstar (1997)). Wilson loops are calculated whose spatial ends have the appropriate symmetries to project onto the different hybrid sectors (see Figure 24). The hybrid potentials obtained can be compared to expectations from excited string models and from bag models. From a Schrödinger equation, masses for the hybrid states can be determined; the particular interest is in ‘exotic’ states which cannot appear in the usual  $Q\bar{Q}$  sector. These states have quantum numbers  $(J = \text{odd})^{-+}$ ,  $(J = \text{even})^{+-}$  or  $0^{--}$ . They are most likely to be visible if their energies are below threshold for Zweig-allowed decay, but it is not clear where this threshold is. Some models expect the hybrid states to decay to an  $S$ -wave heavy-light state and a  $P$ -wave, in which case the threshold is rather higher than for conventional heavyonium decay (for a recent review of expected hybrid phenomenology see Close (1997)).

The hybrid potentials obtained (see Figure 25) are very flat, indicating broad states, closely packed in energy. The lightest mass hybrids from these potentials are close to the threshold described above. The same picture is obtained by calculating the masses of heavy-heavy hybrids directly using NRQCD (Collins

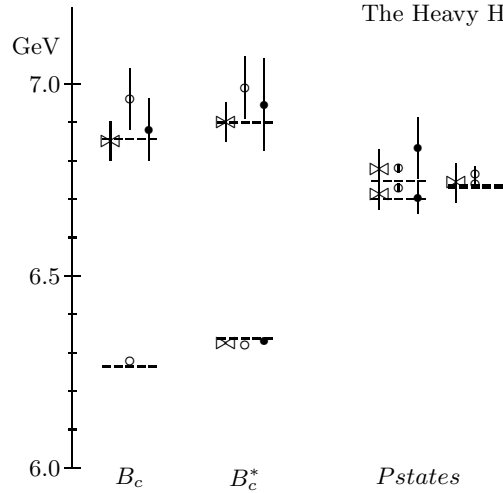


**Fig. 23.** Lattice results for the spectrum of the  $B_c$  system. Open circles indicate NRQCD results on quenched configurations, closed circles those on partially unquenched configurations from the MILC collaboration. Bowties indicate results on quenched configurations using NRQCD for the  $b$  quark and relativistic  $c$  quarks. Error bars are shown where visible and only indicate statistical uncertainties. (Davies *et al* (1996), Shanahan (1997), Gorbahn *et al* (1997)). Dashed lines show results from a recent potential model calculation (Eichten and Quigg (1994)).

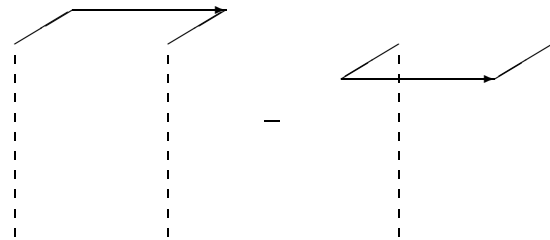


**Fig. 24.** An example of an operator used at the end of a Wilson loop in the calculation of the hybrid ( $H$ ) potential.

(1997b), Manke (1997)). Further work must be done on the spectrum if the states are to be accurately predicted for experimental searches.

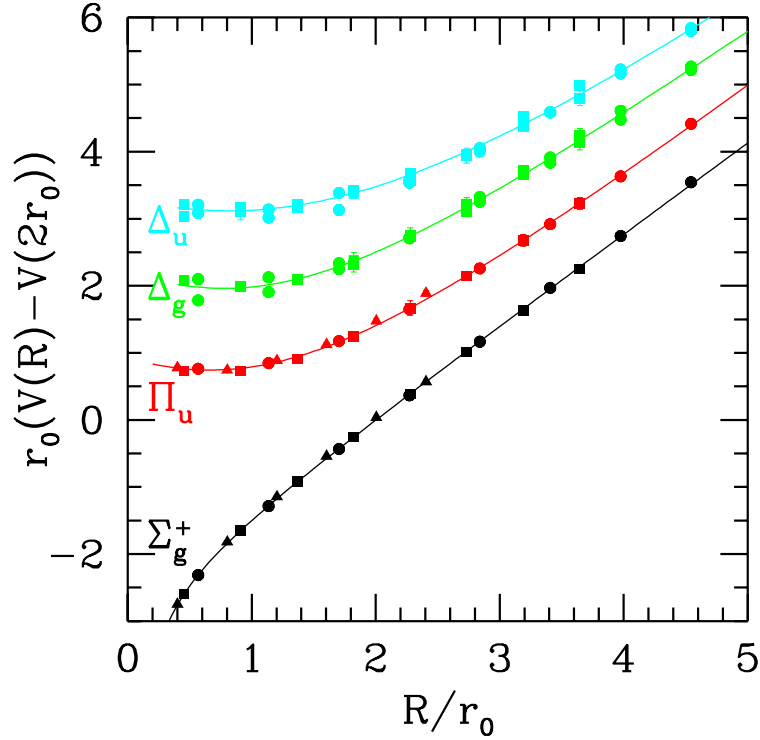


**Fig. 25.** The heavy hybrid potential from a recent lattice calculation (Juge, Kuti and Morningstar (1997)). The  $\Sigma_g^+$  potential is the usual central potential; the  $\Pi$  potential has a gluonic excitation with spin 1 about the  $Q\bar{Q}$  axis and the  $\Delta$  potentials have spin 2.

### 3 The heavy-light spectrum

#### 3.1 Mesons

These are bound states with one heavy valence quark or anti-quark and 1 light anti-quark or quark. The levels show a similar picture to that for the heavy-heavy spectrum with the lightest state the pseudoscalar ( $^1S_0$ ) and close by the vector ( $^3S_1$ ). For charm-light we have pseudoscalars  $c\bar{d} = D^+$ ,  $c\bar{u} = D^0$  and  $c\bar{s} = D_s$ , and vectors,  $D^{*0}$ ,  $D^{*+}$  and  $D_s^*$ . For bottom-light we have pseudoscalars  $b\bar{d} = \bar{B}^0$ ,  $b\bar{u} = B^-$  and  $b\bar{s} = \bar{B}_s$ , and vectors again for each. We shall ignore the distinction (and slight mass difference) between heavy-light mesons containing  $u$  and  $d$  quarks and often just refer to  $D$  and  $B$ . Radially excited  $S$  states,  $D'$  and  $B'$  are about 500 MeV above the ground states and below these come a set of positive parity  $P$  states, denoted by their spins  $D_0^*/B_0^*$ ,  $D_1/B_1$ ,  $D_2^*/B_2^*$  etc. or more generically  $D^{**}$  and  $B^{**}$ . See Figure 26 and The Particle Data Group

(1996).

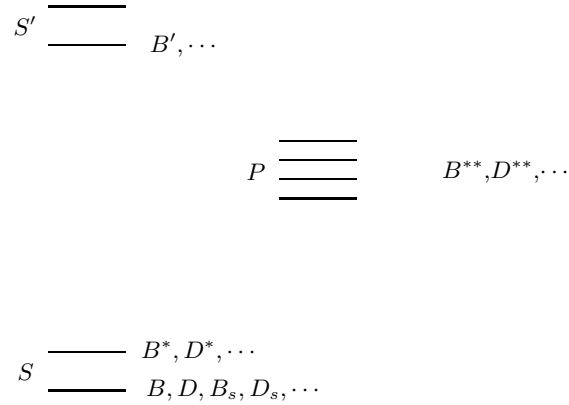


**Fig. 26.** The spectrum of heavy-light mesons.

We do not expect a potential model to work well for the heavy-light spectrum because the light quarks are now relativistic. The heavy quarks are still non-relativistic, however. Taking  $\Lambda_{QCD}$  as a typical QCD momentum scale of a few hundred MeV, we have

$$\begin{aligned} \text{Momentum}_Q &\sim \text{Momentum}_q \sim \Lambda_{QCD} \\ \frac{v_Q}{c} &\sim \frac{\Lambda_{QCD}}{m_Q} \end{aligned}$$

giving  $v_Q \sim 0.1$  for  $b$  in  $B$  and  $0.3$  for  $c$  in  $D$ . This is  $v_Q$ , not  $v_Q^2$ , so the heavy quark is actually more non-relativistic than in heavy-heavy systems.

A useful analysis is provided by Heavy Quark Symmetry (see Neubert (1994) for a review). In the  $m_Q \rightarrow \infty$  limit QCD has an  $[SU(2N_F)]$  symmetry where  $N_F$  is the number of flavours of heavy quark in the theory. This is evident from the NRQCD Lagrangian of equation 22 which, by the arguments above, is appropriate for the heavy quarks here also. As  $m_Q \rightarrow \infty$  the Lagrangian becomes  $\psi^\dagger D_t \psi$  when the quark mass term is removed. Thus the heavy quarks become spinless and any distinction between flavours disappears (apart from the overall

energy level set by the missing mass term). The picture of a heavy-light meson becomes one of a static heavy quark surrounded by a fuzzy cloud of the light degrees of freedom, known as ‘brown muck’, as in Figure 27. Interactions that probe only momentum scales appropriate to the brown muck will not be able to see details of the heavy quark at the centre. Notice that this is a completely different physical picture to that for heavy-heavy mesons.

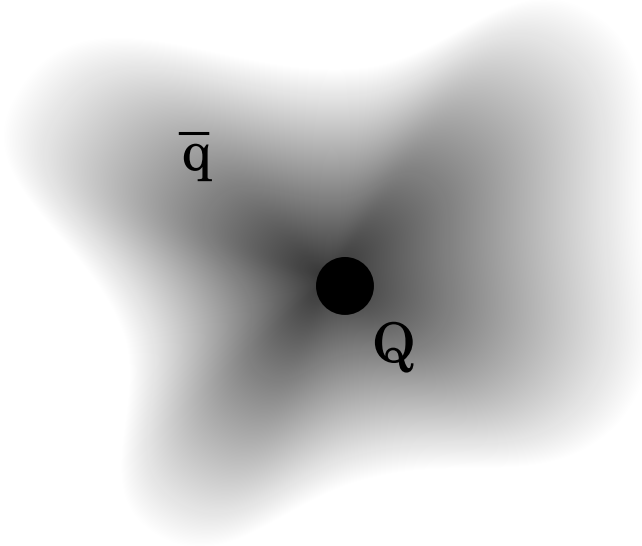


**Fig. 27.** A heavy-light meson in the Heavy Quark Symmetry picture.

From the picture of Figure 27 there is a natural distinction between energy shifts in the spectrum that are caused by something changing for the light degrees of freedom, e.g. a radial or orbital excitation, and those caused by something changing for the heavy quark, such as its flavour or spin. In the first case we expect that radial and orbital excitation energies should be approximately independent of the heavy quark flavour, and in the second case we expect much smaller splittings with strong heavy quark mass dependence between states of different  $\mathbf{S}_Q$ . This hierarchy of splittings is similar to that for heavy-heavy mesons but for different reasons. The  $m_Q$ -independence of the  $1P - 1S$  splitting in heavyonium is an accident; in heavy-light mesons it is the consequence of a symmetry of the non-relativistic effective theory as  $m_Q \rightarrow \infty$ .

A power-counting analysis of the terms in the NRQCD Lagrangian is useful to demonstrate this effect (Ali Khan *et al* (1996)).

$$D_t \sim \mathbf{D} \sim \Lambda_{QCD} \tag{64}$$



from above. Then

$$\frac{\mathbf{D}^2}{2m_Q} \sim \frac{\Lambda_{QCD}^2}{m_Q}. \quad (65)$$

Also

$$\mathbf{A} \sim A_t \rightarrow \mathbf{E}, \mathbf{B} \sim \Lambda_{QCD}^2 \quad (66)$$

and

$$\begin{aligned} \frac{\boldsymbol{\sigma} \cdot \mathbf{B}}{m_Q} &\sim \frac{\Lambda_{QCD}^2}{m_Q} \\ \frac{\boldsymbol{\sigma} \cdot \mathbf{D} \times \mathbf{E}}{m_Q^2} &\sim \frac{\Lambda_{QCD}^3}{m_Q^2} \end{aligned} \quad (67)$$

This shows that, for the heavy-light case, the NRQCD Lagrangian is a  $1/m_Q$  expansion (unlike the heavy-heavy case where terms at different order in  $1/m_Q$  appeared at the same order in  $v_Q^2$ ). The leading order term is the  $D_t$  term and then at the next order come two  $1/m_Q$  terms - the kinetic energy of the heavy quark and the spin coupling to the chromo-magnetic field. These are the first two terms to know about the heavy quark flavour (mass) and its spin. Any splitting that requires this knowledge will appear first at  $1/m_Q$  in an expansion in the inverse heavy quark mass.

The heavy quark spin,  $\mathbf{S}_Q$ , is a good quantum number in the heavy quark limit and so we can classify states according to  $\mathbf{j}_l = \mathbf{J} - \mathbf{S}_Q$ . Each  $\mathbf{j}_l$  state becomes, on the addition of the heavy quark, a doublet with  $J = j_l \pm 1/2$  (Isgur and Wise (1991)). An analogy can be drawn with atomic physics and the decoupling of the nuclear spin as  $m_e/m_N \rightarrow 0$ . The lightest states are the  $L = 0$ ,  $j_l = 1/2$ ,  ${}^3S_1 (D^*, B^*) / {}^1S_0 (D, B)$  doublet. For heavy-light  $P$  states the light quark spin,  $S_q$ , is coupled to the orbital angular momentum to make states of overall spin,  $j_l = 1/2$  ( 2 polarisations ) or  $j_l = 3/2$  ( 4 polarisations). Coupling  $S_Q$  to  $j_l = 3/2$  gives total  $J=2$  ( $B_2^*, D_2^*$ ) and  $J=1$  ( $B_1', D_1'$ ) (8 states altogether). Coupling  $S_Q$  to  $j_l = 1/2$  gives  $J=0$  or  $J=1$  (4 states altogether). Thus in the  $jj$  coupled basis we reproduce the same 12 states as the  $LS$  coupled  ${}^1P_1, {}^3P_{0,1,2}$  multiplet. However, the spin 1 states are a mixture of the  ${}^1P_1$  and  ${}^3P_1$  (with mixing angle  $35^\circ$ ) because of a lack of charge conjugation. In the  $m_Q \rightarrow \infty$  limit only the splittings caused by the light degrees of freedom remain. The  $jj$  basis becomes the correct one and all the  $j_l = 3/2$  states become degenerate but split from all the  $j_l = 1/2$  states. The  $j_l = 3/2$  states are narrow (and therefore visible) because of the high orbital angular momentum required in decays to  $D^{(*)}B^{(*)}\pi$  for  $J=2$ .  $J=1$  can only decay to  $D^*/B^*\pi$  but, having the same  $j_l$  as the  $J=2$  state, has a similar total width (see Figure 28 and Isgur and Wise (1991)).

The difference between the  $j_l + 1/2$  and  $j_l - 1/2$  members of a doublet is a spin flip of the heavy quark. The leading term that gives rise to this in the NRQCD Lagrangian is the  $\boldsymbol{\sigma}_Q \cdot \mathbf{B}$  term, yielding a splitting behaving as  $\lambda \times (\text{spin factors}) \times 1/m_Q$ .  $\lambda$  is an expectation value in the light quark degrees of freedom so the heavy quark mass dependence of the splitting is as  $1/m_Q$  in leading order.

Table 4 shows experimental values for the vector-pseudoscalar splitting (The Particle Data Group (1996)).  $1/m_Q$  behaviour fits very well if we take  $m_c \approx 1.5$  GeV and  $m_b \approx 5$  GeV. We can also consider the strange quark as a heavy quark rather than a light one and add the value for the strange-up/down system, the  $K$  into the Table. This only works moderately well, with  $m_s \approx 0.5$  GeV, say. The coefficient of the  $1/m_Q$  dependence is of order  $0.2 \text{ GeV}^2$ , which is compatible with an expectation value in a light system of  $\Lambda_{QCD}^2$ . Note that the variation with light quark mass between  $u/d$  and  $s$  is very small. It is clear that  $B_c$  cannot be fitted into this heavy-light picture since its expected hyperfine splitting is much larger (see section 2.5).

Splitting	Experiment/ MeV	'Expected' value / MeV
$K^* - K$	398	457
$D^* - D$	141	152
$D_s^* - D_s$	144	
$B^* - B$	46	46
$B_s^* - B_s$	47	
$K_2^*(1430) - K_1(1270)$	154	
$D_2^* - D_1$	37	
$D_{s2}^* - D_{s1}$	38	

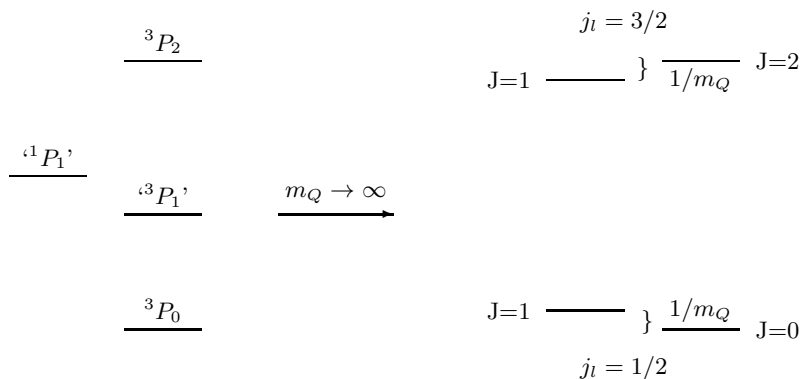
**Table 4.** Hyperfine splittings for different heavy-light systems; the top group for the  $L = 0, j_l = 1/2$  doublet, the lower group for the  $L = 1, j_l = 3/2$  doublet. The final column gives expected values for the  ${}^3S_1 - {}^1S_0$  splitting rescaling from the  $B$  system by the inverse ratio of quark masses given in the text. (The Particle Data Group (1996)).

Table 4 also shows results for the  $L = 1, j_l = 3/2$  doublet from the  $D$  and  $K$  systems (Eichten *et al* (1993)). The ratio of splittings between  $D$  and  $K$  is rather different for this case to the one above, probably showing that the  $K$  is stretching the limits of HQS arguments. Nevertheless, we expect a splitting  $B_2^* - B_1$  of  $m_c/m_b \times (D_2^* - D_1) \sim 12$  MeV. A value of 26 MeV is given in DELPHI (1995) for the  $B_s$ . Experimental results for the  $L = 1, j_l = 1/2$  doublet are not available since these are much broader than the  $j_l = 3/2$  doublet.

In contrast there are several splittings that we expect, from the arguments above, to be controlled by changes in the light quark degrees of freedom and therefore to be independent of the heavy quark mass at leading order. One of these is the splitting between the heavy-strange and heavy-up/down mesons. Experimentally this is satisfied at the 10% level (see Table 5). Other such splittings are those between radially excited  $S$  states and the ground states for which experimental information is very limited ( $B' - B = 580$  MeV (Landua (1997)) and  $D^{*'} - D^* = 630$  MeV (DELPHI (1997b))), and between orbitally excited  $P$  states and the ground  $S$  states, which we discuss below.

Splitting	Experiment / MeV
$D_s - D$	99
$B_s - B$	90

**Table 5.** Experimental values for splittings between heavy-strange and heavy-up/down systems (The Particle Data Group (1996)).



**Fig. 28.** On the left,  $P$  fine structure for a degenerate heavy-heavy system. On the right,  $P$  fine structure for a heavy-light system.

For the orbital splittings between heavy-light  $S$  and  $P$  states we should calculate a splitting between spin-averaged states, to remove the spin-dependent  $1/m_Q$  effects, and make as clear as possible the  $m_Q$ -independent light quark effects. Since  $j_l = 1/2$  states have not been seen, we compare in Table 6 the splitting between the spin-average of the  $j_l = 3/2$   $P$  states and the spin-averaged  $S$  states for  $D$  and  $B$ . Good agreement between the 2 systems is seen. For  $B$  states good spin separation of the  $P$  states is not yet available.

We would also expect the splitting between the  $j_l = 1/2$  and the  $j_l = 3/2$  states to be approximately independent of  $m_Q$  (Isgur (1997)), although the physical spin 1 states will be a mixture of the  $jj$  states away from the  $m_Q \rightarrow \infty$  limit. This cannot be checked experimentally as yet.

### 3.2 Baryons

There is a huge array of baryon states with one heavy quark and two light quarks. Again we can make sense of their masses using Heavy Quark Symmetry arguments. We view the baryon as a static colour source (for the heavy quark) surrounded by a fuzzy light quark system which is made of two light quarks this time instead of a light anti-quark (Falk (1997)).

Splitting	Experiment / MeV
$\overline{K}_p(1368) - \overline{K}(792)$	576
$\overline{D}_p(2445) - \overline{D}(1975)$	470
$\overline{D}_{sp}(2559) - \overline{D}_s(2076)$	483
$B^{**}(5698) - \overline{B}(5313)$	385
$B_s^{**}(5853) - \overline{B}_s(5404)$	449

**Table 6.** Splittings between spin-averaged  $j_l = 3/2$   $P$  states (or experimentally un-separated  $P$  states) and spin-averaged  $S$  states for heavy-light systems (The Particle Data Group (1997)).

We will discuss only the case of zero relative orbital angular momentum. For two different light quarks we can combine the light quark spins to give a total  $S_l$  of 0 or 1. If the light quarks have the same flavour, only  $S_l = 1$  is possible by Fermi statistics, remembering the overall anti-symmetry of the colour wavefunction. Coupling the heavy quark spin then gives the combinations in Table 3.2, with overall spin-parity assignments.

baryon	$Qqq$	$S_l$	$J^P$	mass <sub>c</sub> /MeV	mass <sub>b</sub> /MeV
$\Lambda$	$Q[ud]$	$0^+$	$\frac{1}{2}^+$	2285(1)	5624(9)
$\Sigma$	$Q\{ud\}, uu, dd$	$1^+$	$\frac{1}{2}^+$	2453(1)	5797(8)
$\Sigma^*$	$Q\{ud\}, uu, dd$	$1^+$	$\frac{3}{2}^+$	2519(2)	5853(8)
$\Xi$	$Q[u/ds]$	$0^+$	$\frac{1}{2}^+$	2468(2)	
$\Xi'$	$Q\{u/ds\}$	$1^+$	$\frac{1}{2}^+$	2568(?)	
$\Xi^*$	$Q\{u/ds\}$	$1^+$	$\frac{3}{2}^+$	2645(2)	
$\Omega$	$Qss$	$1^+$	$\frac{1}{2}^+$	2704(4)	
$\Omega^*$	$Qss$	$1^+$	$\frac{3}{2}^+$		

**Table 7.**  $J^P$  possibilities for baryons containing one heavy quark along with two light quarks. The names are given with subscripts  $c$  or  $b$ . Masses are given in the last two columns, taken from The Particle Data Group (1997), DELPHI (1995) for  $\Sigma_b$  and WA89 (1995) for  $\Xi'$ .

Using HQS arguments we would expect the splitting between the spin average of  $\Sigma$  and  $\Sigma^*$  states and the  $\Lambda$  to be independent of  $m_Q$ , since this splitting represents a change in  $j_l$ . We can check this in Table 8, and it works well even when the  $s$  quark is considered as a heavy quark. There is in fact very little room for sub-leading  $1/M_Q$  dependence which can in principle be there ( $\Lambda_{QCD}^2/m_c \sim 50$  MeV). In the last row is given for comparison the splitting between the spin-average of the  $\Xi_c^*$  and  $\Xi_c'$  and the  $\Xi_c$ . This is essentially the same splitting except

for the different light quark content. The answer is significantly different, showing more sensitivity to light quark content than for the mesons (Falk (1997)). The physical  $\Xi'_c$  and  $\Xi_c$  will be mixtures of the HQS states, just like the spin 1 meson  $P$  states, but this should not be a big effect. An equal spacing rule,  $\Omega_c - \Xi'_c = \Xi'_c - \Sigma_c$  holds well.

Splitting	Experiment / MeV
$\overline{\Sigma}_s - \Lambda_s$	203
$\overline{\Sigma}_c - \Lambda_c$	212
$\overline{\Sigma}_b - \Lambda_b$	210
$\overline{\Xi}'_c - \Xi_c$	150

**Table 8.** Experimental values for the splitting between the spin-average of  $\Sigma$  states and the  $\Lambda$  for different heavy quarks including  $s$ . In the last row a comparable splitting is given for the  $\Xi_c$ .

All the fine structure splittings between states of the same  $S_l$  but different  $J$  should behave as  $1/m_Q$ . Table 9 shows the experimental information on this for the  $\Sigma$  baryons. The  $s$  quark fits well into this picture, but the experimental  $\Sigma_b^* - \Sigma$  splitting looks significantly different from the expected value (Falk (1997)). The experimental results need to be confirmed, however. The  $\Xi^* - \Xi'$  splitting agrees well with the  $\Sigma^* - \Sigma$  showing no large  $m_s$  effects here.

Splitting	Experiment / MeV	'Expected' / MeV
$\Sigma_s^* - \Sigma_s$	191	198
$\Sigma_c^* - \Sigma_c$	66	66
$\Sigma_b^* - \Sigma_b$	56	20
$\Xi_c^* - \Xi'_c$	80	

**Table 9.** Splittings between  $\Sigma^*$  and  $\Sigma$  states for different heavy quarks, including  $s$ . The last column gives expected values for  $1/m_Q$  behaviour compared to the splitting for  $c$ .

We can also take splittings between baryons and mesons. The simplest splitting is between the  $\Lambda$  baryons and the  $S$  state mesons. To remove spurious  $m_Q$  dependence we should take the spin-average of the  $^1S_0$  and  $^3S_1$  meson states (Martin and Richard (1987)). Table 10 shows the experimental results; again Heavy Quark Symmetry works much better than might be expected.

HQS yields only the  $m_Q$  dependence of the splittings; it must be combined

Splitting	Experiment / MeV
$\Lambda_s - \overline{K}$	323
$\Lambda_c - \overline{D}$	310
$\Lambda_b - \overline{B}$	310

**Table 10.** The splitting between the  $\Lambda$  baryon and the spin average of  $S$  state heavy-light mesons for different heavy quarks, including  $s$ .

with a non-perturbative method of determining the coefficients of this dependence. QCD sum rules can be invoked here (Neubert (1994)); Lattice QCD provides a better *ab initio* method. We discuss results from lattice QCD in the next subsection.

**Exercise:** Discuss what you would expect for heavy-heavy-light baryons. Take  $Q_1 \neq Q_2$ .

**Exercise:** Compare orbitally excited  $\Lambda_s$  and  $\Lambda_c$  baryons from the Particle Data Tables. What does this lead you to expect for the orbitally excited  $\Lambda_b$ ? (Rosner (1995)).

### 3.3 Direct calculations of the heavy-light spectrum on the lattice

Following the methods described for the heavyonium spectrum, we can calculate the heavy-light spectrum directly using lattice QCD. We must combine a heavy quark propagator with a light anti-quark propagator (or two light quark propagators) to make a meson (baryon) correlation function. This we fit as before to a sum of exponentials to extract ground and excited state energies and masses. In principle some of the excited states can undergo strong decays upsetting this relation, but this does not happen in current lattice simulations.

For hadrons containing a  $b$  quark the best method is probably to use NRQCD for the heavy quark as described for bottomonium in section 2.3. Because of the different power-counting rules for the heavy-light case, the Lagrangian used can be different to that for heavyonium. For example, a consistent calculation to  $\mathcal{O}(1/m_Q)$  would include  $D_t$ ,  $\mathbf{D}^2/2m_Q$  and  $\boldsymbol{\sigma} \cdot \mathbf{B}/2m_Q$  terms (tadpole-improved as before). In fact for the heavy-light case the spectrum can be calculated in the static limit with simply the  $D_t$  term, because the light quark provides the kinetic energy. In this case, of course, only states of a given  $j_l$  are obtained with no hyperfine splittings. The static limit is very cheap computationally but much noisier (Lepage (1992)) than NRQCD even at very large  $m_Q$  and for this reason it may be more accurate to obtain static results from the limit of NRQCD calculations. For hadrons containing a  $c$  quark, we will discuss results using the heavy Wilson (SW) action.

Since we do not have a potential model in principle to guide our intuition, it is more difficult to think of good smearing functions for heavy-light mesons.

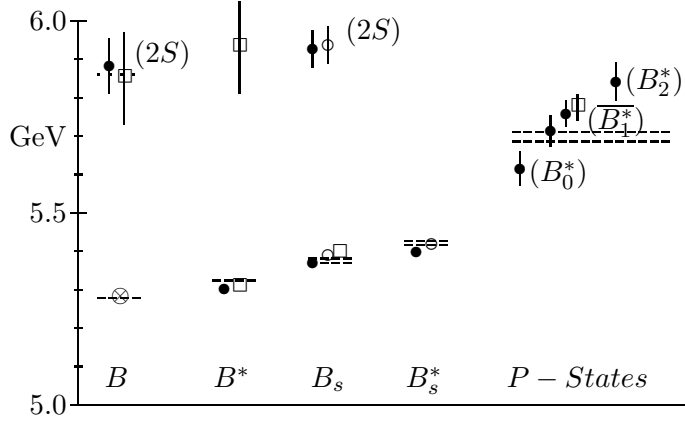


**Fig. 29.** The  $B$  spectrum from lattice QCD using NRQCD for the  $b$  quark. Circles are in the quenched approximation; open circles use  $m_s$  from  $K$  and closed circles,  $m_s$  from  $K^*$ . Squares are results on configurations with  $n_f = 2$  dynamical fermions. Experimental results (The Particle Data Group (1997)) are given by dashed horizontal lines. The  $B$  meson mass is fixed to its experimental value in all cases (Ali Khan (1997)).

A lot of effort has been put into this for mesons in the static case (Duncan *et al* (1995), Draper *et al* (1995)) to ameliorate the noise problems. Again, the smearing does not affect the values of masses obtained, but a good smearing can reduce the errors. In fact potential-model type wavefunctions (much broader than for heavyonium) do work reasonably well (Duncan *et al* (1995), Ali Khan *et al* (1996)), used as a source for the heavy quark, as do gauge-invariant smearings typical of light hadron calculations (UKQCD (1996b)). The light anti-quark for the meson is taken to have a delta function source. Alternatively both propagators can be smeared, and for baryons it is certainly a good idea for all the propagators to be smeared (UKQCD (1996b)).

The meson operators are similar to those for heavyonium -  $\psi_Q^\dagger \Omega \phi \chi_q^\dagger$ . For the NRQCD heavy quark case  $\Omega$  is a  $2 \times 2$  matrix in spin space and only 2 components are taken from the 4-component light quark. The colors of heavy quark and light anti-quark are matched for a colour singlet. The baryon operators need an anti-symmetric colour combination, and the light quark propagators combined with appropriate spins (UKQCD (1996b)). For example the  $A_Q$  operator (with smearing factors,  $\phi$  suppressed) is:

$$\mathcal{O} = \epsilon^{ABC} (\chi_{q_1}^{A\dagger} \mathcal{C} \gamma_5 \chi_{q_2}^B) \psi_Q^{\dagger C} \quad (68)$$

where  $\mathcal{C}$  is the charge conjugation matrix.

In principle, having calculated the bottomonium spectrum in NRQCD as in section 2.3 on a given set of gluon configurations, we can determine  $a^{-1}$

and the bare  $b$  quark mass,  $m_b$ , and the calculation of the  $B$  spectrum should have no parameters to tune. Unfortunately this is not true in the quenched approximation. The disagreement with experiment shown in Figure 18 makes it clear that the  $a^{-1}$  fixed from the  $\Upsilon$  spectrum would be  $\sim 20\%$  different to that from  $M_\rho$ , because of the different momentum scales appropriate to the two systems. Heavy-light systems are much closer to light hadrons in these terms than to heavyonium. For the best quenched results we really need to use a value for  $a^{-1}$  from the heavy-light system itself, but the lack of experimental information on  $P$  states makes this hard, since the obvious quantity to use is the  $1P - 1S$  splitting. Usually  $a^{-1}$  is taken instead from light hadron spectroscopy. Large statistical and systematic uncertainties there then give a rather large error.

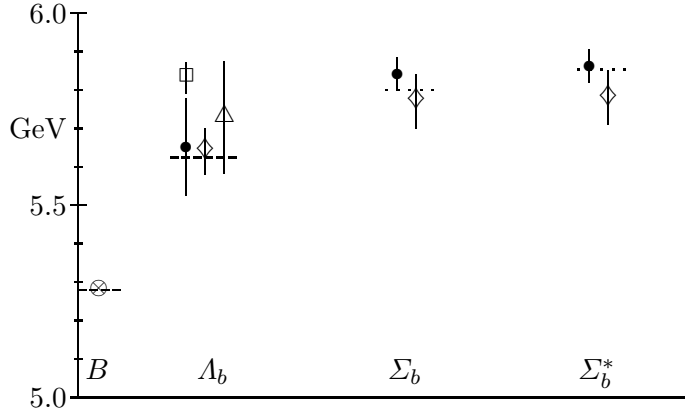


**Fig. 30.** Masses of baryons containing one  $b$  quark from lattice QCD. Circles use NRQCD for the  $b$  quark in the quenched approximation, the box uses NRQCD on configurations with  $n_f = 2$  flavours of dynamical fermions. Triangles (Alexandrou *et al* (1994b)) use Wilson fermions, and diamonds the SW action (UKQCD (1996b)) extrapolating from the region of the charm quark, again in the quenched approximation. Experimental results are given by horizontal lines (The Particle Data Group (1997), DELPHI (1995)). (Ali Khan (1997)).

This creates a problem with the bare  $b$  quark mass,  $m_b$ , since it was fixed in bottomonium using  $a^{-1}$  from that system. It should be fixed again in heavy-light systems using the kinetic mass of, say, the  $B$ . This is difficult to extract accurately because  $B$ s are lighter than  $\Upsilon$ s.  $E(p) - E(0)$  is larger for the  $B$  than the  $\Upsilon$  so the noise in the meson correlation function at finite momentum  $p$  (set by  $E(0)$ ) is worse. An alternative is to calculate the usual energy at zero momentum,  $E_B(0)$ , and apply the energy shift per quark in lattice units calculated for heavyonium to get  $m_{BA}$  (Ali Khan *et al* (1996), Collins *et al* (1996b)).



These problems mean that the heavy-light spectrum cannot be as accurately calculated as that of heavyonium. Once dynamical fermions are included sufficiently well to mimic the real world there can only be one value of  $a^{-1}$  and  $m_{b/c}$ . We are a long way from this point at present, however. It is not even possible to perform consistent  $n_f$  extrapolations (to  $n_f = 3$ ?) of the heavy-light spectrum from results at  $n_f = 0$  and 2 (Collins *et al* (1996b) and in preparation). For heavyonium differences in methods of fixing  $a^{-1}$  disappeared on this extrapolation but this is not currently true for heavy-light mesons and shows the presence of systematic errors.

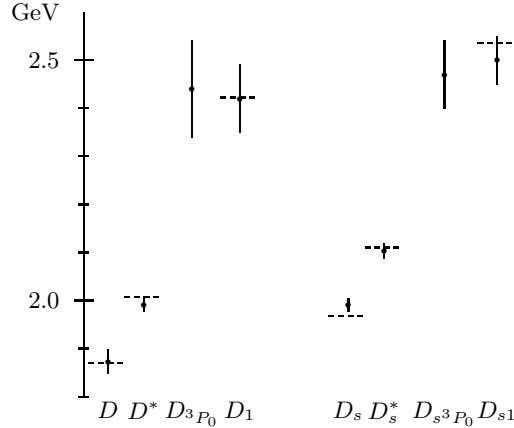
Another difficulty with the heavy-light spectrum is that of fixing the light quark mass. This is a problem shared with light hadron calculations (Weingarten (1997), Montvay and Münster (1994)). The  $B$  and  $D$  calculations must be done with several different light quark masses far from the physical  $u/d$  masses and the results extrapolated to the chiral limit. This inevitably causes an increase in statistical and systematic errors. For the  $B_s$  and  $D_s$ , it is possible to interpolate to the  $s$  quark mass although there are ambiguities in fixing that, again possibly arising from the quenched approximation (see, for example, Gupta and Bhattacharya (1997)).

Figure 29 shows the  $b$ -light meson spectrum using NRQCD for the  $b$  quark, fixing  $m_b$  from the  $B$  mass and  $a^{-1}$  from  $M_\rho$  (from a recent review by Ali Khan (1997)). The overall agreement with experiment is good. The  $B^* - B$  splitting is too small, however, both on quenched and on partially unquenched configurations. As before, this may be a quenching effect and/or it may arise from radiative corrections to  $c_4$  beyond tadpole-improvement (see the discussion for heavyonium). The problems with fixing  $m_s$  are clear. The  $P$  states still have rather large error bars but the ordering,  $B_0^*, B_1, B_2^*$  is becoming clear in the lattice results (in disagreement with some expectations (Isgur (1997))). The spin 1  $P$  states cannot be clearly separated as yet. Experimental results on the  $P$  states are likewise uncertain. Results at a different value of the lattice spacing are compared in Hein (1997).

Figure 30 shows the  $b$ -light baryon spectrum using NRQCD for the  $b$  quark (Ali Khan (1997)). Agreement with experiment is again reasonably good, although the  $\Lambda_b$  baryon is apparently too heavy on the partially unquenched configurations. The baryons are probably rather susceptible to finite volume effects, and further work is definitely needed on bigger volumes. The  $\Sigma^* - \Sigma$  splitting is too small in the quenched approximation, which does not seem surprising by now.

Results in the static limit for mesons and baryons, for the states that still exist there, are similar to those from NRQCD but have been in the past less accurate - see Peisa and Michael (1997), UKQCD (1996a), Duncan *et al* (1995), Alexandrou *et al* (1994a) and Duncan *et al* (1993). A comparison is made in Figure 30 to results using heavy Wilson quarks for the  $b$ . This will be discussed further below.

Arguments earlier showing that the heavy quarks are more non-relativistic in heavy-light than heavy-heavy does mean that NRQCD should work better for



**Fig. 31.** The  $D$  meson spectrum from lattice QCD using a tadpole-improved SW action in the quenched approximation. Masses are fixed relative to the spin average of the  $D_s$  and the  $D_s^*$  (Boyle (1997a)). Horizontal dashed lines mark the experimental results (The Particle Data Group (1996)).

the  $D$  than for the  $\psi$  but currently results are only available for  $S$ -states at one value of the lattice spacing (Hein (1997)). For  $c$ -light mesons and baryons the SW action (or other heavy Wilson action) is probably to be preferred even in this case. Figure 31 shows a recent  $D$  spectrum using the tadpole-improved SW action for the  $c$  quark presented here by Peter Boyle (Boyle (1997a)). The agreement with experiment is encouraging but it has not been possible to extract all the  $P$  fine structure as yet, and errors bars there are still rather large. Uncertainties in how to fix  $a^{-1}$  and  $m_c$  are the same here as for the  $b$  case above. In the Figure  $a^{-1}$  is taken from light hadron spectroscopy. Results have been compared at two values of the lattice spacing (Boyle (1997b)). No  $D$  spectrum is available from unquenched configurations as yet.

Figure 32 shows the  $c$ -light baryon spectrum using the SW action for the  $c$  quark but this time not tadpole-improved (UKQCD (1996b)). Agreement with experiment for the  $m_Q$ -independent splittings is reasonable but the hyperfine splittings are much too small. At least a part of this comes from the lack of tadpole-improvement since this directly affects the ' $\sigma_Q \cdot \mathbf{B}$ ' term in this formalism.

It is tempting to try extrapolating to the  $b$  quark from the  $c$  quark using the results from the SW action and HQS arguments to set the  $m_Q$ -dependence of splittings. This is probably fine for splittings which have little or no  $m_Q$  dependence, in which case extrapolation is not really necessary. We have seen that there are several splittings for which the leading behaviour is a constant and for which there seems almost no sub-leading dependence on  $m_Q$ . For the splittings that have strong  $m_Q$  dependence it is much more difficult to pick up

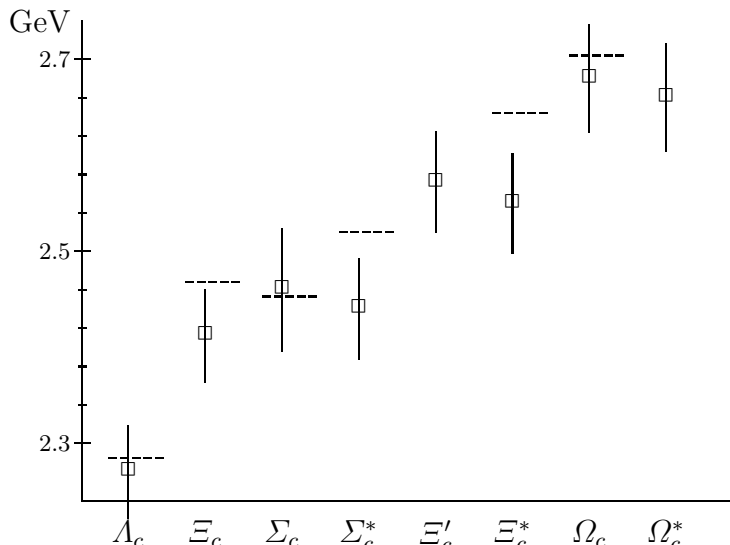


**Fig. 32.** The spectrum of baryons containing one  $c$  quark obtained on the lattice using the SW action for the  $c$  quark in the quenched approximation (UKQCD (1996b)). The horizontal dashed lines give experimental results (The Particle Data Group (1997)).

this dependence from the small  $m_Q$  side than from the large. Figure 30 compares results from NRQCD with extrapolated results from unimproved Wilson quarks (Alexandrou *et al* (1994b)) and SW quarks (UKQCD (1996b)). In the latter case the low value obtained for the hyperfine  $\Sigma^* - \Sigma$  splitting becomes worse on extrapolation. In principle the SW action is safer for heavy-light mesons than for heavy-heavy as was discussed in section 2.4. and so calculations at the  $b$  itself can and should be done with this method (Simone *et al* (1997)).

Finally lattice QCD calculations do not have to restrict themselves to the physical quark masses but can explore the whole heavy quark region. This enables a fit to the dependence on  $m_Q$  (or on the pseudoscalar meson mass, say) of a range of splittings. The coefficients of this dependence are then non-perturbative parameters of a heavy quark expansion which can be made use of in other heavy quark relations. The values of the coefficients can be compared to expectations of powers of  $\Lambda_{QCD}$  and to QCD sum rule results (Collins *et al* (1996b), Collins (1997a), Gimenez *et al* (1997)).

## 4 Conclusions

There has been a lot of progress in heavy hadron spectroscopy using the techniques of lattice QCD in recent years, converting the qualitative understanding of potential models and Heavy Quark Symmetry into clear numerical results that test QCD.

Further work is still needed to bring down systematic errors. Upsilon spectroscopy is the most accurate at present. Here, more calculations need to be done with a non-relativistic action which includes next-to-leading spin-dependent terms and radiative corrections to leading terms. Finite volume effects must be studied for radially excited states. More accuracy is needed on dynamical configurations with several different values of  $n_f$  to allow for a clear extrapolation of fine structure to the real world. A prediction for the  $\Upsilon - \eta_b$  mass at the 10% level is a realisable goal with current calculations.

The charmonium spectrum is more complete experimentally but more work is needed on the lattice using heavy Wilson actions to reduce statistical and systematic errors (e.g. from  $D^4$  terms). Calculations on configurations with dynamical fermions are required for extrapolations to compare to experiment.

In the heavy-light sector statistical and systematic errors are inevitably larger and these must be reduced if we are to get a clear picture of the fine structure and radial excitations from the lattice that are now being seen experimentally. Analyses of scaling as the lattice spacing is changed and finite volume studies for these systems are still at an early stage. In the next few years a clearer picture will emerge of the effect of the quenched approximation on ‘softer’ momentum systems such as light and heavy-light hadrons and ambiguities of scale setting and quark mass fixing should be removed.

Finally, as noted at the beginning, we are also interested in matrix elements for radiative and weak decays of heavy hadrons, particularly those which are important for the experimental  $B$  physics programme. Calculations of these are being done on the lattice also, using the techniques described here for the spectrum. These calculations are much harder and accurate spectrum results will be a prerequisite for accurate matrix elements.

#### Acknowledgements

I thank the organisers for a very enjoyable school and the following for help in preparing these lectures: Arifa Ali Khan, Gunnar Bali, Peter Boyle, Sara Collins, Joachim Hein, Henning Hoerber, Peter Lepage, Paul McCallum, Colin Morningstar, Junko Shigemitsu, John Sloan and Achim Spitz. A lot of the work described here was supported by PPARC and NATO under grant CRG 941259. I am grateful to the Institute for Theoretical Physics, UCSB, for hospitality and to the Leverhulme Trust and the Fulbright Commission for funding while these lectures were being written up.

## References

- ALEPH collaboration (1997): Phys. Lett. **B402**, 213.
- C. Alexandrou, S. Güsken, F. Jegerlehner, K. Schilling and R. Sommer (1994a): Nucl. Phys. **B414**, 815.
- C. Alexandrou, A. Borrelli, S. Güsken, F. Jegerlehner, K. Schilling, G. Siegert and R. Sommer (1994b): Phys. Lett. **B337**, 340.
- M. G. Alford, T. R. Klassen and G. P. Lepage (1997): Nucl. Phys. B (Proc. Suppl.) **53**, 861.

- A. Ali Khan in : Proceedings of LAT97, Edinburgh, July 1997, Nucl. Phys. B (Proc. Suppl.) to appear.
- A. Ali Khan, C. Davies, S. Collins, J. Sloan and J. Shigemitsu (1996): Phys. Rev. D**53**, 6433.
- S. Aoki *et al* (1997): Nucl. Phys. B (Proc. Suppl. **53**), 355.
- T. Appelquist, M. Dine and I. Muzinich (1978): Phys. Rev. D**17**, 2074.
- G. Bali, K. Schilling and A. Wachter (1997a): hep-lat/9703019, Phys. Rev. D (in press).
- G. Bali, K. Schilling and A. Wachter (1997b): Phys. Rev. D**55**, 5309.
- G. Bali and K. Schilling (1992): Phys. Rev. D**46**, 2636; *ibid* D**47**, (1993) 661.
- A. Barchielli, N. Brambilla and G. Prosperini (1990): Nuovo Cimento **103A**, no. 1, 59.
- G. Bodwin, E. Braaten and P. Lepage (1995): Phys. Rev. D**51**, 1125.
- P. A. Boyle (1997a): in Nucl. Phys. B (Proc. Suppl. **53**), 398.
- P. A. Boyle (1997b): in Proceedings of LAT97, Edinburgh, July 1997, Nucl. Phys. B (Proc. Suppl.) to appear.
- W. Büchmüller and S.-H. H. Tye (1981): Phys. Rev. D**24**, 132.
- F. Butler, H. Chen, J. Sexton, A. Vaccarino and D. Weingarten (1994): Nucl. Phys. B**430**, 179.
- Y.-Q. Chen, Y. P. Kuang and R. J. Oakes (1995): Phys. Rev. D**52**, 264.
- F. Close (1979): *An Introduction to Quarks and Partons*, Academic Press.
- F. Close (1997): in Proceedings of LAT97, Edinburgh, July 1997, Nucl. Phys. B (Proc. Suppl.), to appear.
- S. Collins (1997): Nucl. Phys. B (Proc. Suppl. **53**), 389.
- S. Collins (1997b): in Proceedings of LAT97, Edinburgh, July 1997, Nucl. Phys. B (Proc. Suppl.), to appear.
- S. Collins, R. G. Edwards, U. M. Heller and J. Sloan (1996a): Nucl. Phys. B (Proc. Suppl. **47**), 455.
- S. Collins, U. Heller, J. Sloan, J. Shigemitsu, A. Ali Khan and C. Davies (1996b): Phys. Rev. D**54**, 5777.
- C. T. H. Davies (1997): in Proceedings of the International Workshop on Lattice QCD on Parallel Computers, Nucl. Phys. B (Proc. Suppl.), in press, hep-lat/9705039 and in Proceedings of LAT97, Edinburgh, July 1997, Nucl. Phys. B (Proc. Suppl.), to appear.
- C. T. H. Davies, K. Hornbostel, A. Langnau, G. P. Lepage, A. Lidsey, J. Shigemitsu and J. Sloan (1994a): Phys. Rev. D**50**, 6963.
- C. T. H. Davies, K. Hornbostel, A. Langnau, G. P. Lepage, A. Lidsey, C. Morningstar, J. Shigemitsu and J. Sloan (1994b): Phys. Rev. Lett. **73**, 2654.
- C. T. H. Davies, K. Hornbostel, G. P. Lepage, A. Lidsey, J. Shigemitsu and J. Sloan (1995a): Phys. Lett. B**345**, 42.
- C. T. H. Davies, K. Hornbostel, G. P. Lepage, A. Lidsey, J. Shigemitsu and J. Sloan (1995b): Phys. Rev. D**52**, 6519.
- C. T. H. Davies, K. Hornbostel, G. P. Lepage, A. Lidsey, J. Shigemitsu and J. Sloan (1996): Phys. Lett. B**382**, 131.
- C. T. H. Davies, K. Hornbostel, G. P. Lepage, P. McCallum, J. Shigemitsu and J. Sloan (1997): Phys. Rev. D**56**, 2755.
- P. de Forcrand and J. Stack (1985): Phys. Rev. Lett. **55**, 1254.
- DELPHI collaboration (M. Feindt) (1995): Invited talk at HADRON'95, CERN-PPE-95-139.
- DELPHI collaboration (1997a): Phys. Lett. B**398**, 207.

- DELPHI collaboration (1997b): Contribution to EPS-97 conference, pa-01,#452, available at <http://wwwcn.cern.ch/pubxx/www/delsec/conferences/jerusalem>.
- T. Draper, C. McNeile and C. Nenkov (1995): Nucl. Phys. B (Proc. Suppl. **42**), 325.
- T. Draper and C. McNeile (1996): Nucl. Phys. B (Proc. Suppl. **47**), 429.
- A. Duncan, E. Eichten, A. El-Khadra, J. Flynn, B. Hill and H. Thacker (1993): Nucl. Phys. (Proc. Suppl. **30**), 433.
- A. Duncan, E. Eichten, J. Flynn, B. Hill, G. Hockney and H. Thacker (1995): Phys. Rev. **D51**, 5101.
- E852, D. R. Thompson *et al* (1997): Phys. Rev. Lett. **79**, 1630.
- E. Eichten (1980): Phys. Rev. **D22**, 1819.
- E. Eichten, K. Gottfried, T. Kinoshita, J. Kogut, K. D. Lane and T.-M. Yan (1975): Phys. Rev. Lett. **34**, 369.
- E. Eichten, K. Gottfried, T. Kinoshita, K. D. Lane and T. M. Yan (1978): Phys. Rev. **D17**, 3090 and *ibid* **D21** (1980), 203.
- E. Eichten and F. Feinberg (1981): Phys. Rev. **D23**, 2724.
- E. Eichten and B. Hill (1990): Phys. Lett. **B243**, 427.
- E. Eichten, C. Hill and C. Quigg (1993): Phys. Rev. Lett. **71**, 4116.
- E. Eichten and C. Quigg (1994): Phys. Rev. **D49**, 5845.
- A. X. El-Khadra and B. P. Mertens (1995): Nucl. Phys. B (Proc. Suppl. **42**), 406.
- A. X. El-Khadra, A. S. Kronfeld and P. B. Mackenzie (1997): Phys. Rev. **D55**, 3933.
- A. Falk (1997): hep-ph/9707295.
- A. F. Falk, B. Grinstein and M. E. Luke (1991): Nucl. Phys. B **357**, 185.
- S. S. Gershtein, V. V. Kiselev, A. K. Likhoded and A. V. Tkabladze (1995): Phys. Rev. **D51**, 3613.
- V. Gimenez, G. Martinelli and C. Sachrajda (1997): Nucl. Phys. **B486**, 227.
- M. Gorbahn, C. T. H. Davies, G. P. Lepage, J. Shigemitsu and J. Sloan (1997): in preparation.
- A. K. Grant, J. L. Rosner and E. Rynes (1993): Phys. Rev. **D47**, 1981.
- B. Grinstein and I. Rothstein (1996): Phys. Lett. **B385**, 265.
- D. Gromes (1977): Nucl. Phys. **B131**, 80.
- D. Gromes (1984): Z. Phys. **C22**, 265.
- D. Gromes (1988): Phys. Lett. **B202**, 262.
- H. Grosse and A. Martin (1980): Phys. Rep. **60C**, 341.
- R. Gupta and T. Bhattacharya (1997): Phys. Rev. **D55**, 7203.
- G. Heatlie, C. T. Sachrajda, G. Martinelli, C. Pittori and G. C. Rossi (1991): Nucl. Phys. **B352**, 266.
- J. Hein (1997): in Proceedings of LAT97, Edinburgh, July 1997, Nucl. Phys. B (Proc. Suppl.) to appear.
- A. B. Henriques, B. H. Kellett and R. G. Moorhouse (1976): Phys. Lett. **B64**, 85.
- A. Huntley and C. Michael (1986): Nucl. Phys. **B270**, 123.
- A. Huntley and C. Michael (1987): Nucl. Phys. **B286**, 211.
- N. Isgur (1997): preprint JLAB-THY-97-26.
- N. Isgur and M. B. Wise (1991): Phys. Lett. **B66**, 1130.
- C. Itzykson and J.-B. Zuber (1980): *Quantum Field Theory*, McGraw Hill.
- A. S. Kronfeld (1997): Nucl. Phys. B (Proc. Suppl. **53**), 401.
- K. J. Juge, J. Kuti and C. J. Morningstar (1997): in Proceedings of LAT97, Edinburgh, July 1997, Nucl. Phys. B (Proc. Suppl.), to appear.
- W. Kwong and J. L. Rosner (1988): Phys. Rev. **D38**, 279.
- R. Landua (1997): Review talk in Proceedings of ICHEP'96, Warsaw, World Scientific.

- G. P. Lepage (1989): *From Action to Answers*, World Scientific.
- G. P. Lepage (1992): Nucl. Phys. B (Proc. Suppl. **26**), 45.
- G. P. Lepage (1996): Lectures given at the 1996 Schladming Winter School, World Scientific.
- G. P. Lepage (1997): in Proceedings of Lattice QCD on Parallel Computers, Tsukuba, Nucl. Phys. B (Proc. Suppl.) in press, hep-lat/9707026.
- G. P. Lepage and P. B. Mackenzie (1993): Phys. Rev. D**48**, 2250.
- G. P. Lepage, L. Magnea, C. Nakhleh, U. Magnea and K. Hornbostel (1992): Phys. Rev. D**46**, 4052.
- M. Lüscher, S. Sint, R. Sommer, P. Weisz and U. Wolff (1997): Nucl. Phys. B**491**, 323.
- T. Manke (1997): in Proceedings of LAT97, Edinburgh, July 1997, Nucl. Phys. B (Proc. Suppl.), to appear.
- T. Manke, I. T. Drummond, R. R. Horgan and H. P. Shanahan (1997): Phys. Lett. B**408**, 308.
- A. Martin (1980): Phys. Lett. B**93**, 338.
- A. Martin and J.-M. Richard (1987): Phys. Lett. B**185**, 426.
- C. Michael and P. E. L. Rakow (1985): Nucl. Phys. B**256**, 640.
- I. Montvay and G. Münster (1994): *Quantum Fields on a Lattice*, Cambridge University Press.
- C. Morningstar (1994): Phys. Rev. D**50**, 5902.
- M. Neubert (1994): Phys. Rep. **245**, 259
- S. Ono, A. Sanda and N. Törnqvist (1986): Phys. Rev. D**34**, 186.
- The Particle Data Group (1996), R. M. Barnett *et al*
- The Particle Data Group (1997): updated particle tables at <http://pdg.lbl.gov/>. Phys. Rev. D **54**, 1.
- S. J. Perantonis and C. Michael (1990): Nucl. Phys. B**347**, 854.
- M. Peskin (1983): in 11th SLAC Summer Institute, SLAC Report PUB 3273.
- J. Peisa and C. Michael (1997): in Proceedings of LAT97, Edinburgh, July 1997, Nucl. Phys. B (Proc. Suppl.) to appear.
- C. Quigg (1997a): Physics Today, Vol. **50** no. 5, 20.
- C. Quigg (1997b): hep-ph/9707493.
- C. Quigg and J. L. Rosner (1977): Phys. Lett. **71B**, 153.
- C. Quigg and J. L. Rosner (1979): Phys. Rep. **56C**, 167.
- P. A. Rapidis *et al* (1977): Phys. Rev. Lett. **39**, 526.
- J. Richardson (1979): Phys. Lett. B**82**, 272.
- J. Rosner (1995): hep-ph/9501291.
- H. J. Schnitzer (1975): Phys. Rev. Lett. **35**, 1540.
- SESAM collaboration, U. Glässner, S. Güsken, H. Hoerber, T. Lippert, G. Ritzenhöfer, K. Schilling, G. Siegert, A. Spitz and A. Wachter (1996): Phys. Lett. B**383**, 98.
- SESAM collaboration, N. Eicker, Th. Lippert, K. Schilling, A. Spitz, J. Fingberg, S. Güsken, H. Hoerber and J. Viehoff (1997): hep-lat/9709002.
- H. Shanahan (1997): in Proceedings of LAT97, Edinburgh, July 1997, Nucl. Phys. B (Proc. Suppl.), to appear.
- B. Sheikholeslami and R. Wohlert (1985): Nucl. Phys. B**259**, 572.
- J. Simone *et al* (1997): in Proceedings of LAT97, Edinburgh, July 1997, Nucl. Phys. B (Proc. Suppl.), to appear.
- R. Sommer (1994): Nucl. Phys. B**411** 839.
- R. Sommer (1997): these Proceedings.

- A. Spitz (1997) in: Proceedings of LAT97, Edinburgh, July 1997, Nucl. Phys. B (Proc. Suppl.), to appear.
- B. A. Thacker and G. P. Lepage (1991): Phys. Rev. D**43**, 196.
- H. B. Thacker, E. Eichten and J. C. Sexton (1988): Nucl. Phys. B (Proc. Suppl. **4**), 234.
- H. Trottier (1997a): Phys. Rev. D**55**, 6844.
- H. Trottier (1997b) in: Proceedings of LAT97, Edinburgh, July 1997, Nucl. Phys. B (Proc. Suppl.), to appear.
- UKQCD collaboration, S. P. Booth *et al* (1992a): Phys. Lett. B**284**, 377.
- UKQCD collaboration, S. P. Booth, D. S. Henty, A. Hulsebos, A. C. Irving, C. Michael and P. W. Stephenson (1992b): Phys. Lett. B**294**, 385.
- UKQCD collaboration, A. K. Ewing *et al* (1996a): Phys Rev. D **54**, 3526.
- UKQCD collaboration, K. C. Bowler *et al* (1996b): Phys Rev. D **54**, 3619.
- UKQCD collaboration, presented by R. D. Kenway (1997): Nucl. Phys. B (Proc. Suppl. **53**), 209.
- WA89 (R. Werding) (1995) : Proceedings of ICHEP'94, Glasgow, IOP Publishing.
- D. Weingarten (1997): these Proceedings.